Case Studies in Construction Materials 16 (2022) e01050

Contents lists available at ScienceDirect

Case Studies in Construction Materials

journal homepage: www.elsevier.com/locate/cscm

Case study

Effect of pores on the mechanical and durability properties on high strength recycled fine aggregate mortar

Rebeca Martínez-García [a,*], M.I. Sánchez de Rojas [b], P. Jagadesh [c], Fernando López-Gayarre [d], Julia M. Morán-del-Pozo [e], Andrés Juan-Valdes [e]

[a] Department of Mining Technology, Topography and Structures, University of León. Campus de Vegazana s/n, 24071 León, Spain
[b] Eduardo Torroja Institute for Construction Science, UEX-CSIC Partnering Unit, C/ Serrano Galvache, 28033 Madrid, Spain
[c] Department of Civil Engineering, Coimbatore Institute of Technology, Coimbatore 641014, Tamil Nadu, India
[d] Department of Construction, Campus de Gijón, University of Oviedo, 33203 Gijón, Spain
[e] Department of Agricultural Engineering and Sciences, University of León, Avenida de Portugal 41, 24071 León, Spain

ARTICLE INFO

Keywords:
Recycled fine aggregate
Mortar
Mechanical
Durability
Microscopic studies
Pores

ABSTRACT

Larger consumption of natural fine aggregates (NFA) leads to an increase in cost, energy, and negative environmental impact. On the contrary, the larger production of construction waste results in the generation of recycled fine aggregate (RFA), which requires safe disposal. The aim of study, is to the hunt for such alternatives, compares the mortar mechanical and durability properties with and without RFA. High strength mortar specimens were produced with mix proportion as 1:3 using RFA as partial replacement for NFA as 0%, 25%, 50% and 100%. The mechanical and durability performance of all specimens was assessed in the terms of compressive strength, flexural strength, water absorption and mercury intrusion porosimetry. Mechanical performance is confirmed by microscopic studies. The main results display that the mortar with 25% of RFA, performed better, which are related to pore structures and their distribution. It is noted that the, pores also increase with the increase in RFA content. The effect of pores on the strength and their relationships are assessed.

1. Introduction

The boom in urban development and industrialization has also led to the generation of construction and demolition waste (C&DW), to be relocated as waste or reused as recycled aggregates. Researchers estimated that aggregates consumption, in general, was around 37,400 metric tons per year in 2010, with the possibility of increasing to 51.7 billion metric tons in 2019 [1]. The high consumption of natural aggregates would have an impact on the damage of ecosystems, while waste and residues could have a much more sustainable destination if properly sorted. The construction sector is the largest producer of waste in the European Union and therefore, the European Parliament established that at least 70% of construction and demolition waste (C&DW) should be recycled as an effective measure until 2020, in all countries that make up the Union. This regulation governs the proper procedures for removing, transporting, storing, treating, and disposing of these wastes [2]. Three types of recycled aggregates can be produced in plants for this purpose: recycled concrete aggregates (RCA), mostly composed of concrete and mortar waste; recycled masonry aggregates (RMA), many from

* Corresponding author.
E-mail addresses: rmartg@unileon.es (R. Martínez-García), srojas@ietcc.csic.es (M.I. Sánchez de Rojas), jaga.86@gmail.com (P. Jagadesh), gayarre@uniovi.es (F. López-Gayarre), julia.moran@unileon.es, juan@unileon.es (J.M. Morán-del-Pozo), andres.juan@unileon.es (A. Juan-Valdes).

https://doi.org/10.1016/j.cscm.2022.e01050
Received 20 February 2022; Received in revised form 22 March 2022; Accepted 3 April 2022
Available online 12 April 2022

recycled ceramic blocks [3–5] and finally, mixed recycled aggregates (MRA), composed of waste building materials. The target assigned to C&DW was achieved in 2016: 90% in mineral fraction recovery rates in Europe and 79% in Spain.

Despite this, the strategy of reusing and recycling of this set of waste has not been fully exploited, according to what is reflected by the indicators in the analytical framework related to the circular economy: in 2016 The contribution of recycled aggregates (RA) to natural aggregates was 8% in Europe and 1% in Spain. The European Directive includes backfilling but, this practice does not allow preserving the value of the materials, therefore it is not suitable for the circular economy. The lack of confidence in the quality of these materials, the absence of specific regulations, and the low price of natural aggregates have had an adverse effect on the efficient management of C&DW materials, as a consequence, the European Commission approved the "Protocol for the management of construction and demolition waste in the European Union, 2016 [6]" and the "Guidelines for waste audits prior to demolition and renovation works of buildings, 2018 [7]". These documents are attempting to provide the authorities with a methodology to achieve the goal set in the related Directive, institutionalizing the practice of selective demolition, the task of segregating the different components and handling them individually, giving these wastes the character of secondary raw material, in a circular economy in which products, materials, and resources are kept within the system as long as possible and waste generation is minimized [8]. Utilization of Natural Fine Aggregate (NFA) in conventional mortar/concrete, plays vital role in mechanical and durability performance. But the extraction of NFA from environment not only creates negative impact but also increase the cost. Hence, there is need of suitable replacement material like RFA in mortar/concrete.

Although, large natural coarse aggregates can be reused without difficulty [5,9] and so many studies are done in it, the same cannot be said for Natural Fine Aggregates (NFA). Evangelista et al., 2005 [10] show that RFA has features and behavior that are very dissimilar from those of NFA. Because of the way it is manufactured, the shape of RFA is irregular, seemingly with high roughness and surface area. Additionally, its mineralogical composition is very rich in calcium or siliceous oxide and cement. Noticeably, the coating of hydrate absorbs water. Zhao et al., 2015a [11] show that the amount of linked hydrate in the RFA is dissimilar for each segment and, accordingly, the water absorption coefficient of the RFA is also different. The workability of mortar is also strongly influenced by the moisture from the RFA. When the RFA is replaced in the mortar, the strength of the mortar can decrease by as much as 60% of the initial value for mortar without RFA [12]. Zhao et al., 2015a [11] show an important effect of the finest fraction (less than 0.63 mm) of the RFA since it produces the most disciplining effect on the mechanical properties of mortars. RA Concrete with high strength and better performance is examined by incorporation of supplementary cementitious materials is reported in literatures [3–5]. Fresh concrete properties of concrete with RA shows higher value than the concrete with natural aggregate [13]. Even multiple use of RA in self-compacting concrete is tested by Abed et al., 2020 [14].

There are two phases absorbed in RA, Viz., Natural aggregate phase, and Old hardened cement mortar paste. More porous characteristics of RA are due to the second phase (old cement paste) in RA [15]. The Presence of adhered mortar on the surface of aggregate can influence the density, water absorption, sulfate content, strength, and consistency of aggregates [16]. This high porosity nature generates, an important characteristic of the system in which it presents called water absorption [17]. An Increase in cement mortar content with RFA increases the water absorption [18]. And also, the presence of RFA prolongs the mixing time and affects the properties [19]. Limited studies are available in literature in the usage of RFA because, greater surface area, higher porosity, and complex composition, which will lead to deterioration in the cement-based material performances [19]. One of the well-known factors with respect to RA is the higher water to cement ratio when compared to the conventional mixture [19] which leads to negative impacts on properties.

To overcome the above problems, the RA at saturated-surface-dry or moisture state has been suggested to be used in mortar or concrete. One such recommended method followed by many researchers is pre-saturation of RFA which will balance the water requirement [19], but nevertheless, there are some drawbacks. First, the potential release of water of saturated RFA will lead to bleeding in the system leading to deformation of hardened properties of the system [20], [21]. Second, the efficiency of RFA is decreased due to the saturation process and its additional requirement for the process [22].

Still, the aggregates are typically incapable to absorb the complete additional water while the mixture is still in the fresh state [20]. In the study by Poon et al., 2004 [20], dry RA makes high initial workability due to a provisional increase of the real water content. Several authors [23,24] summarized that the amount of extra water according to 80% and 90% of 24 h water absorption of RA would be acceptable for both workability and compressive strength. But this extra water is varied due to the processing technique adopted for the preparation of RFA and the quality of adhered mortar to it.

Application of high strength mortar solves filling problems and helps to produce more gorgeous surface in terms of esthetic appearances [25]. Repair and rehabilitation of reinforced concrete structures requires high strength mortar [26]. Addition of fiber to high strength mortar has wide applications including coatings, pavements, repair of hydraulic structures patches, prefabrications, thin sheets, projected mortar, wall cladding, earthquakes resistant structures, reinforcement of slabs, bridge decks, etc.,[27].

In order to understand the behavior of RFA, it is essential to study their porosity and their pore size distribution, not only in the old paste but also in the new paste apart from the interaction of old and new paste [28]. The most extensively used method to study the pore structure and its distribution is mercury intrusion porosimetry [MIP] [29], [30], [31]. Nonetheless, MIP has restrictions in determining the actual pore diameter below 3 nm and above 375 μm and distribution of pore sizes, because the pore size is too small and it is distributed unevenly or too isolated to be filled by mercury [28]. But MIP tranquil has a greater capacity for the evaluation of total porosity and a characteristic of pore size [32]. Limited studies are available in the literature [33,34] for the application of MIP in mortar with RA.

Results reported that the replacement of natural aggregates by RA increases the porosity with an increase in RA content. It is reported that the RA alters pore size distribution with higher intrusion volumes in pores which diameters larger than 0.01 μm [33,34]. Previous studies [35,36] on replacement of natural aggregate by RA indicates that there is a correlation between the volume of RA and

pore size. However, there are a greater number of studies on the replacement of NFA by RFA in concrete which is available in the literature [37–39] and only a few studies on replacement of NFA by RFA in mortar are reported [40–43].

Despite regulatory limitations, RFA does have some applications. For example, in European Standard UNE-EN 13139/AC:2004 [44], RFA is allowable in masonry mortar manufacturing. Limited studies are available with respect to RFA, 100% replacement of RFA, and application of MIP separately in the literature. Hence, the main objective of this present research is to evaluate the mechanical and durable properties of mortar with RFA. And also, this research becomes vital, in the application purpose for the industrial sector and in academia.

2. Materials and methods

2.1. Materials

2.1.1. Cement and water

CEM-Type III/A 42.5 N/SR is used as cement in this examination as per UNE-EN 197-1:2011 [45]. Physical and chemical features of binder are tabulated in Table 1. Vicat apparatus is used to determine the initial and final setting time as per UNE-EN-196-3:2017 [46]. Water as per UNE-EN 196-1:2018 [47] is used for the making of all mortars.

2.1.2. Fine aggregates

Control Mortar (CM) is manufactured with standard sand with the particle size in the range of 0.075–2 mm as per CEN standardization. RFA is supplied from the recycling plant, located in the Province of Leon, Spain with size of particle in the range of 0.08–2 mm as per UNE-EN 196-1:2018 [47] without any pretreatment of RFA. RFA is characterized as per UNE-EN 13139/AC:2004 [44] and their requirements are verified. Particle size distribution of RFA and its limit as per the standards UNE-EN-933-2:1996 [48] and UNE-EN-933-1:2012 [49] is shown in Fig. 1. Several properties of aggregate not only provide stabilization for the mortar but also provide the suitable distribution of particles which result in an increase in density. In literature, several researchers reported that the distribution of different size of particles of aggregates is one of the important properties determining the concrete or mortar properties [50].

To remove the impurities adhered to the RFA, and to improve the RFA quality, it is washed in manufacturing plant itself. RFA received from plant is subjected to sieving in the laboratory to remove the particles larger than 4 mm and different sizes of RFA is shown in Fig. 2. Different proportions of recycled content existing in FRA is shown in Table 2, consisting of natural stones, concrete, tiles and bricks as a major part and minor part are gypsum, glass and bituminous. It is observed that these proportions are conforms with standards. A physical and mechanical characteristic of RFA is tabulated in Table 3 as per EHE-08 and its acceptable limits are verified.

Particle size distribution of RFA is similar to that of normal sand as shown in Fig. 1 and its properties are similar as reported by previous researchers [12,44]. Water absorption of RFA is somewhat lower than the limits prescribed by EHE-08 [51]. Impurities are removed by pretreatment process of RFA which leads to reduction in water absorption. Water absorption capacity of RFA depends on the type and quantity of cement mortar attached to it and also quantity of ceramic materials contained in it.

2.1.3. Mix proportions

A mix with the volumetric proportion of cement: sand as 1:3 is prepared and it is cast as per UNE-EN 196-1:2018 [47] standard. Totally four mixes of mortar are prepared, in which three mixes made of RFA replacements and the balanced one is Controlled Mix (CM). RFA is used as replacement for NFA as 25%, 50% and 100% for preparation of RFA blended mortars. Mortar flow is kept as 134 $\pm$ 4 mm in order to maintain the consistence index of mortars as constant and to determine the water to cement (W/C) ratio as per UNE-EB 196-1:2018 [47] and UNE-EN 1015-3:2000/A2:2007 [54]. Increase in replacement of NFA by RFA results in increase in W/C ratio is noted from Table 4 and this is due to higher water absorption nature of RFA.

Increase in W/C ratio with increase in RFA content is already reported by previous studies [1,8,50]. W/C ratio plays a vital role in performance of RA blended mortar [55,56]. Proportions of ingredients used in this investigation are tabulated in Table 4. Mortars are

Table 1
Portland cement CEM Type III/A 42.5 N/SR characteristics.

Chemical composition	Value (wt%)	Limit (wt%) [45]
Clinker (SiO_2, Fe_2O_3, Al_2O_3, CaO, MgO and SO_3)	54	35–64
Blast-furnace slag	41	36–65
Minor components	5	$\leq$5
LOI (Loss on ignition)	1.97	$\leq$5
Physical characteristics		[48]
Le Chatelier (mm)	1.5	$\leq$5
Initial setting time (min)	195	$\geq$60
Final setting time (min)	295	$\geq$60
Mechanical characteristics		[44]
Compressive strength (MPa) 2 days	20.1	$\geq$13.5
Compressive strength (MPa) 28 days	56.6	$\leq$42.5 and $\leq$62.5

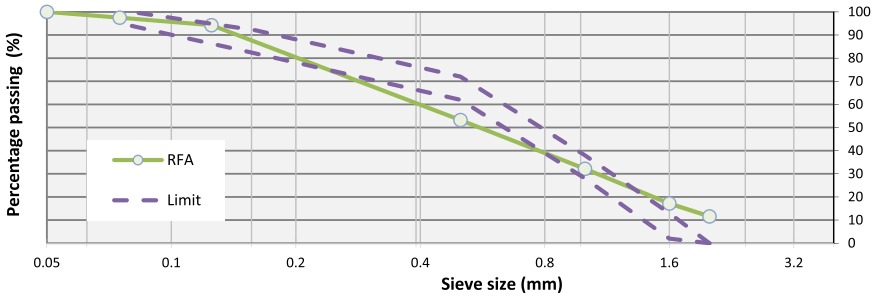

Fig. 1. Particle size distribution of recycled fine aggregate.

Fig. 2. Recycled Fine Aggregate with different sizes.

Table 2
Composition of the urban origin RFA.

Parameter	Standard	Value	Limit EHE-08 [51]
Composition (%)	EN 933-1:2012 [49]		
Floating particles (%)		0	≤1
Gypsum and impurities (%)		0.04	≤1
Concrete (%)		70.7	–
Natural stone (%)		27	–
Bricks and tiles (%)		2.3	≤5
Bituminous mat (%)		0	≤1
Glass (%)		0	≤1

Table 3
Physical and mechanical characterization of the urban origin RFA.

Parameter	Standard	Value	Limit EHE-08 [51]
Flakiness index (%)	EN 933-3:2012 [52]	5.7	≤35
Density and absorption	EN 1097-6:2014 [53]		
P_a (apparent density) (Mg/m^3)		2.52	–
P_{od} (oven dry density) (Mg/m^3)		1.94	–
P_{ssd} (saturated surface dry density) (Mg/m^3)		2.17	–
WA^{24} (water absorption) (%)		4.8	≤5

prepared as per UNE-EN-1:2018 [47]. In order to achieve sustainability in RFA blended mortar, the superplasticizers are not used and hence, the W/C ratio increases with increase in RFA content. Another reason is to understand the effect of pore size and pore size distribution on the mechanical and water absorption properties of RFA blended mortar without chemical admixture leads to natural settlement or moment of RFA particles inside the system. This will lead to the formation of pores and pores distribution without influence of any external chemical factor [57], [58]. In this research, four mix is made with 0%, 25%, 50%, 75% and 100% of NFA

Table 4
Mix proportion (kg/m^3) of FRA blended mortar.

Content (m^3)	CM	CM 25	CM 50	CM 100
Cement (kg)	450	450	450	450
Water (kg)	189	225	243	279
Natural sand (kg)	1350	1012.5	675	0
Fine recycled aggregate (kg)	0	337.5	675	1350
W/C ratio	0.42	0.5	0.54	0.62
Consistency	134	134	134	134.5
Theoretical density (kg/m^3)	1989	2024.5	2043	2213.5

replaced by RFA named as CM, CM25, CM50 and CM100. The design strength of mortar mix for similar ratio as observed from literatures is higher than 50 MPa for 28 days compressive strength is observed from literatures [59,60].

2.2. Methods

2.2.1. Mechanical properties

High strength mortar was tested for mechanical properties like density, compressive strength and flexural strength at 7, 28 and 90 days as shown in Fig. 3. The density of RFA mortars were determined for different curing periods as per UNE-EN 1015-10:2000/A1:2007 [61]. Mechanical properties for high strength recycled aggregate mortar were determined as per UNE-EN 1015-11:2020 [50] and UNE-EN 196-1:2018 [47].

2.2.2. Microstructure characteristics

Undistributed samples are subjected to microscopic studies in order to understand the pores, microcracks, propagation of microcracks, and the possible interaction between the aggregates and mortar [62]. Microstudies were done at different ages of curing on small undistributed samples. This heading consists of sample preparation of each microscopic studies and instrument used for it. Microscopic studies like Scanning Electron Microscope (SEM), Back Scattered Electron (BSE) microscope and Energy Dispersive X-ray analyzer (EDX) are used. For SEM analysis, the sample is prepared in a manner that there is no surface defects or cracks in the surface and it is verified visually. Before the sample is subjected to SEM analysis, first the hydration reaction sample should be stopped. Hydration is arrested with acetone and samples are dried at room temperature under nitrogen gas stream [63]. Samples are coated with carbon using sputter coater for 30 s and they are fixed to metallic sample holder using a bi-adhesive graphite foil. To guarantee conductivity, the surface of the sample must be metallized with carbon. SEM analysis are used to examine the surface morphology of sample exposed.

2.2.3. Pore characteristics

2.2.3.1. Capillary water absorption test. To determine the water absorption due to capillary action the methodology and procedures are followed in European Standard UNE-EN 1015-18 [64]. An Increase in the mass of specimen after immersion due to the fact that capillarity through the prismatic specimen cross-section in contact with a water surface is measured. The Test was performed on the three specimens per mix after curing for 28 days. Water absorption coefficient due to capillary action was estimated and the water absorption rate expressed over a period of time between 10 min and 90 min.

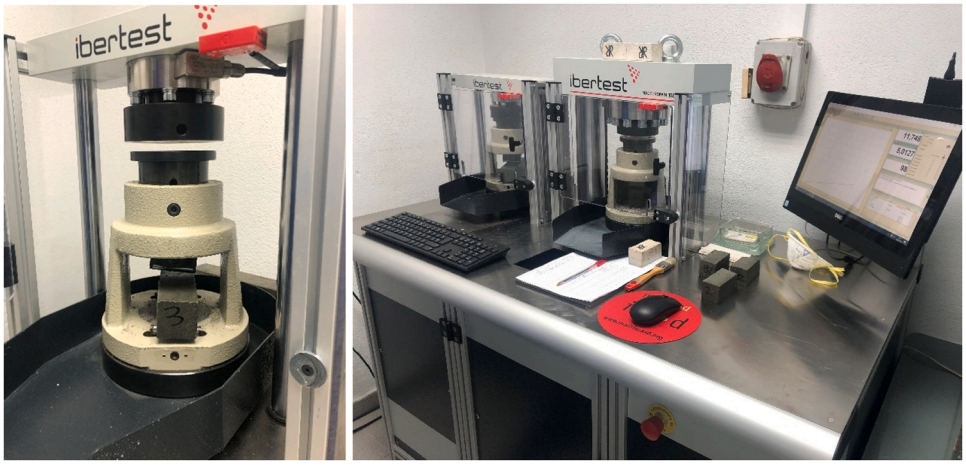

Fig. 3. Compressive and flexural strength test of RFA mortar.

$$C = 0.1 \quad (M2 - M1)kg/(m^2.min^{0.5}) \tag{1}$$

Where:*M1: mass of the specimen immersed for 10 minM2: mass of the specimen immersed for 90 min*

2.2.3.2. Water absorption test. Water absorption test is used to determine the water absorption, density and porosity accessible to water are determined by the method of water absorption by vacuum and hydrostatic weighing of the test specimens after drying them to constant weight at low humidity, once saturated in water the mortar samples according to the UNE-EN 83980:2014 [65].

2.2.3.3. Mercury porosity test. Mercury intrusion porosimetry (MIP) test samples, with a 1–2 gram weight and average of 1 cm length, were extracted from the crushed specimens. Controlling the sample dimensions and mass, errors caused by hysteresis and moisture entrapment during MIP test [66]. Porosity was quantified on Micromeritics Autopore IV 9500 mercury porosimeter designed to measure pore diameters from 0.006 to 175 μm and operate at pressures up to 33,000 psi (227.5 MPa).

3. Results and discussion

3.1. Mechanical properties

The mechanical properties of this present research are already published by the same author [58] and their relationship between the percentage of replacement are discussed. However, to understand the role of pores in RFA blended mortar, the relationship between strength, density, and W/C ratio, which is reported in Figs. 4 and 5 is necessary. W/C ratio and density play an essential role in determining the different types of pores in a system.

Predominately, it is observed that with an increase in W/C ratio, the strength and density decreased and it is also reported in previous studies [67]. Donza et al., 2002 [68] reported that the water demand of mortar increased for crushed RFA. And another study [19], stated that different particle sizes of RFA, increases the water demand of mortar. Most RFA is in an angular shape, having a higher surface area, requires more water to make workable. Apart from this, the different sizes of RFA require more water to achieve the same workability [19]. Even some authors [69], reported that they had irregular shapes with a minimum variation of particle size also increases the water requirement of mortar.

Strength properties decrease initially for 7 and 28 days for all replacement of NFA by RFA. In order to maintain similar workability of mortar with RFA, water content increased with an increase in RFA content in the mix, and also it is higher than the control mortar. Due to higher water content, the water particles are evaporated and density starts decreasing. It is claimed that different particle size of RFA requires more water to reduce the friction between different particle sizes and also requires more water to achieve same consistency. Due to different shape of FRA particles (i.e., mostly irregular shape) requires extra water. Another reason stated in the literature [19], is the smaller particle size, has more surface area, and requires more amount of water to wet the surface and makes it workable. More space is created between the particles in the structure of the mortar, which leads to less connection, thus decreasing the mechanical properties. Zhao et al., 2014 [70] demonstrate that porosity is not the only reason affecting the compressive strength of mortar.

An Increase in curing period results in an increase in mechanical properties is observed in Figs. 4 and 5 with a reduction in density. This increase in mechanical properties is due to two factors. First, the material properties of RFA, and second the evolution of RFA. The Angular shape and the bound old cement paste coated are the main reasons for the difference in the features of the RFA: i.e., reduction in density and rise in water absorption. Many studies have obtained similar finding sand stated that these results are due to above characteristics [39], [71]. Longer period of curing or exposure of RA, may be suspectable to carbonation. Carbonation does not change the granulometry of the NFA but, by absorbing Carbon dioxide, the RFA properties are modified and it becomes denser [72]. Thus, the occurrence of old cement paste in the RFA alters their chemical features comparative to those of the NFA. The cement content in the RFA depends on the manufacturing process of RFA and it is straightly connected to the size of RFA [71]. Characteristics of cement mortar paste adhered to RFA are directly related to the origin of recycled concrete [73].

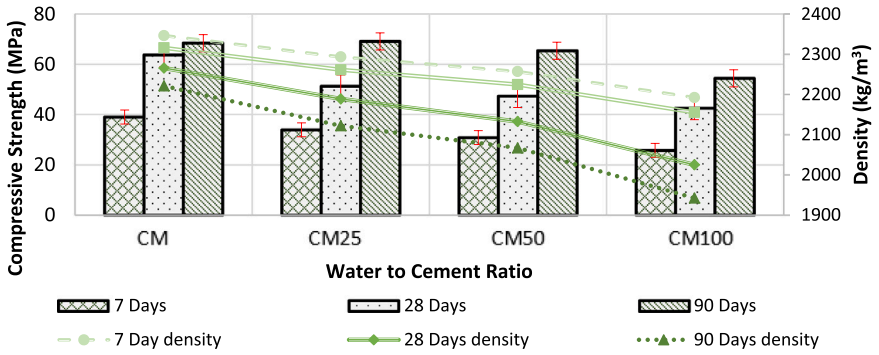

Fig. 4. Relationship between W/C ratio, compressive strength, and density at various curing periods for control mortar and mortar with RFA.

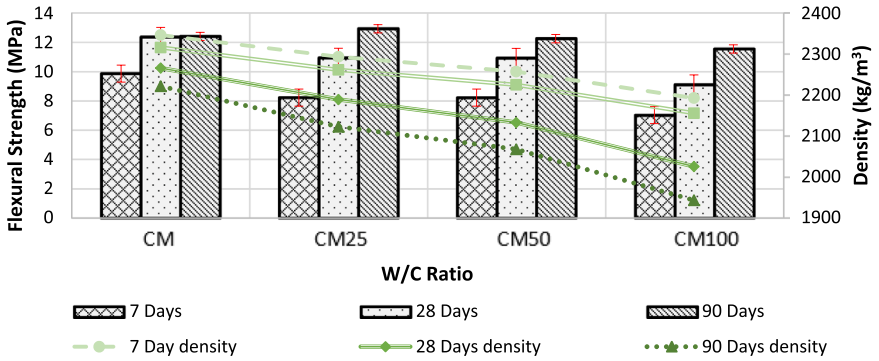

Fig. 5. Relationship between W/C ratio, flexural strength, and density at various curing periods for control mortar and mortar with RFA.

3.2. Microscopic studies

The SEM study reveals the morphology of the mortars tested and the possible changes due to the use of RFA compared to FRA at two curing ages. As can be seen in the micro-photographs of the Figs. 4, 5, 6 and 7, no significant changes are observed in the morphology of the mortars when RFA is incorporated. Mortars with RFA have small pores compared to the CM sample, except for mortar with 100% RFA. These results will be discussed together with those obtained by MIP. Fig. 6 shows the OPC mortar at the two test ages. It is

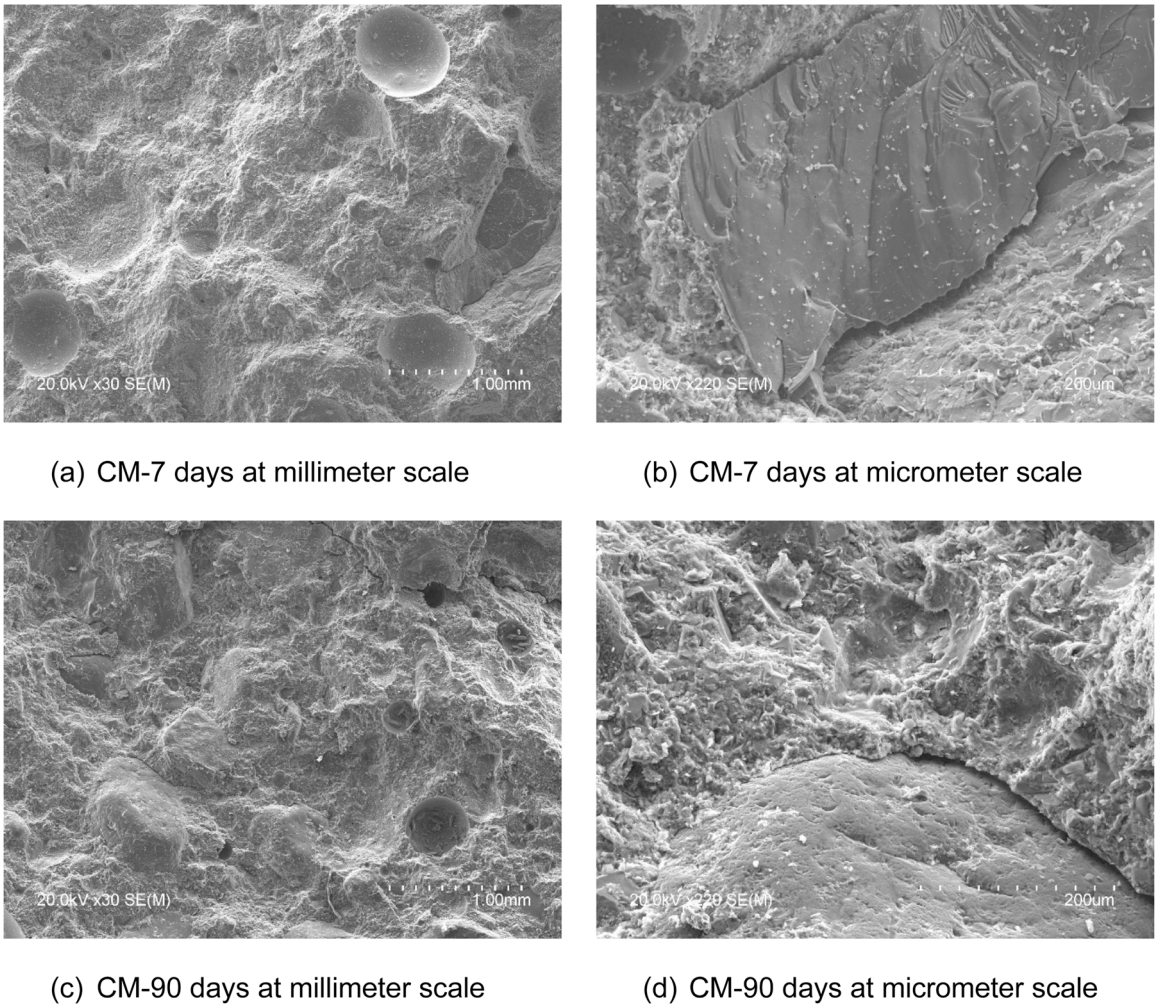

Fig. 6. SEM analysis for control mortar (CM) at 7 and 90 days.

observed on a micrometer scale, that the size of the pores reduces with the increase in the curing age (in Fig. 6(a) and 6(c)), this is known due to the formation of a greater number of hydrated products, which makes the cement mortar matrix be homogeneous and denser. Furthermore, a good adhesion between the natural sand and the cement matrix is observed, which is the reason for its good mechanical behavior (Fig. 6d).

The presence of elemental composition is determined by using EDS. In Fig. 6, it is observed that there are two different element compositions observed in Fig. 6(b) and 6(d). Sand grains are clearly visible with a higher element of silica is observed in Fig. 6(b), which indicates the denser matrix in the NFA grain. And the presence of calcium and silica in Fig. 6(b) indicates the formation of hydration products. Fig. 6(d) shows the presence of fine aggregates and the formation of hydration products, especially Calcium Silicate Hydrate (CSH).

In the mortars with a lower percentage of RFA (Fig. 7), there was densification of the ITZ due to greater number of hydrated phases and lower porosity. The efficacy of freeing water from within the porous RFA to the cement matrix depends on the suction force, which in turn depends on the porosity and relative humidity of cement paste [74]. As reported by Zou et al., 2019 [75] capillary pore pressure increases linearly with the decrease of relative humidity. Note the existence of small pores in the cement paste as well as in the RFA mortar, also there is a reduction in the pore size of the aggregate for the cement paste. This variance in pore size aided in the release of water from the pore aggregate, because the smaller the pore diameter, the greater is the suction force for the water to be freed from the pores of the porous aggregate. Thus, the small pores (<4 nm in diameter) maintain for a longer period occupied with water and in their saturated condition may be filled with hydration products which, following the release of water, remain with hydration products [74]. Hence, there are strength feature increases slowly with increase in curing period is owing to the formation of hydration products in the inner pores in aggregates and in cement paste. Due to increasing in curing period, there is a reduction in number of pores and pore diameter in millimeter scale observed in Fig. 7(a) and (c).

EDS analyzes carried out on the binder paste show Calcium/Silica (C/S) relationships between 1.9 and 2.7. EDS analysis of Fig. 7

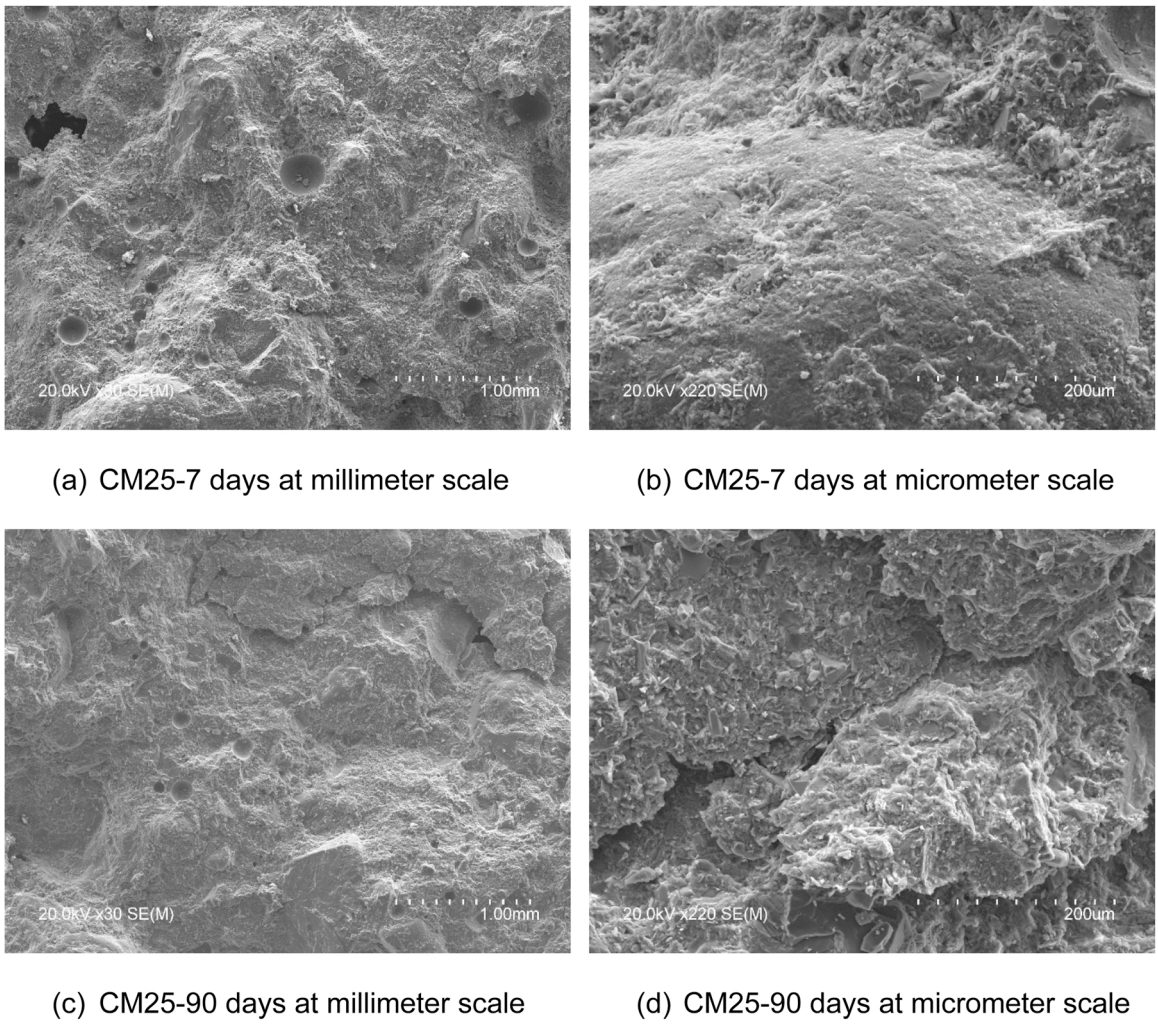

Fig. 7. SEM analysis for CM25 at 7 and 90 days.

(b), indicates that the presence of aluminum as 11.61, higher the presence of aluminum leads to incorporation of aluminum to CSH gel, results in formation of CASH [64]. EDS analyzes carried out on the paste show that the main elements are silicon and calcium, which form the CSH gels, with C/S ratios of 2.85, which is too high, which indicates that it could be an anhydrous product, and very low of 1.9. Analyzes carried out on the aggregate in the image shows that the majority of elements are silicon, aluminum and potassium, which corresponds to the presence of recycled sand. It can be seen how the aggregate present in this image corresponds to the natural aggregate of the silica or also a grain of silica present in RFA. The analyzes carried out in Fig. 7(d) in this image highlights that the recycled sand is possibly present in it, in whose composition aluminum, silicon, calcium and potassium mainly take part, it is cohesive with the hydrated cement paste, which presents Ca/Si from 2.3 to 2.6. These dense hydration products are contributing to improving the mechanical and durability properties of mortar.

Formation of a greater number of pores with an increase in RFA is observed in Fig. 8(a) at millimeter-scale apart from hydrated and not hydrated particles of old mortar. On a micrometer scale, a large number of hydrated and not hydrated particles are clearly visible in Fig. 8(b). The hydration products which are formed to bind the old cement mortar particles are not enough too denser, results pores in it leads to crack. At 90 days of curing, the size of pores formed is reduced and the propagation of cracks is through these pores is confirmed in Fig. 8(c). At a micrometer scale, a greater number of old finer hydrated products are visible and it is detached from cement matrix are also confirmed in Fig. 8(d). Porosity is a first-order variable that inversely affects the mechanical properties of cementations composites. The higher the porosity, the lower the compressive strength. The presence of pores in the samples may be due to pores not filled by the solid paste compounds, irregularly or spherical shape shaped are owing to entrained air trapped during mixing [76]. EDS analyzes in Fig. 8(b), the aggregate present is of the siliceous type, and the hydrated cement has a C/S ratio of 2.3–2.56. It is difficult to identify the RFA; it could be distinguished by higher potassium content at the initial curing period. Fig. 8(d), indicates that hydrated cement paste has very high C/S ratios such as 2.65 and in some places, the ratios are reduced to 2.1. The presence of potassium content indicates the presence of RFA.

In Fig. 9(a), the size of pores is increased when compared to the previous replacement at a millimeter scale. At a micrometer scale,

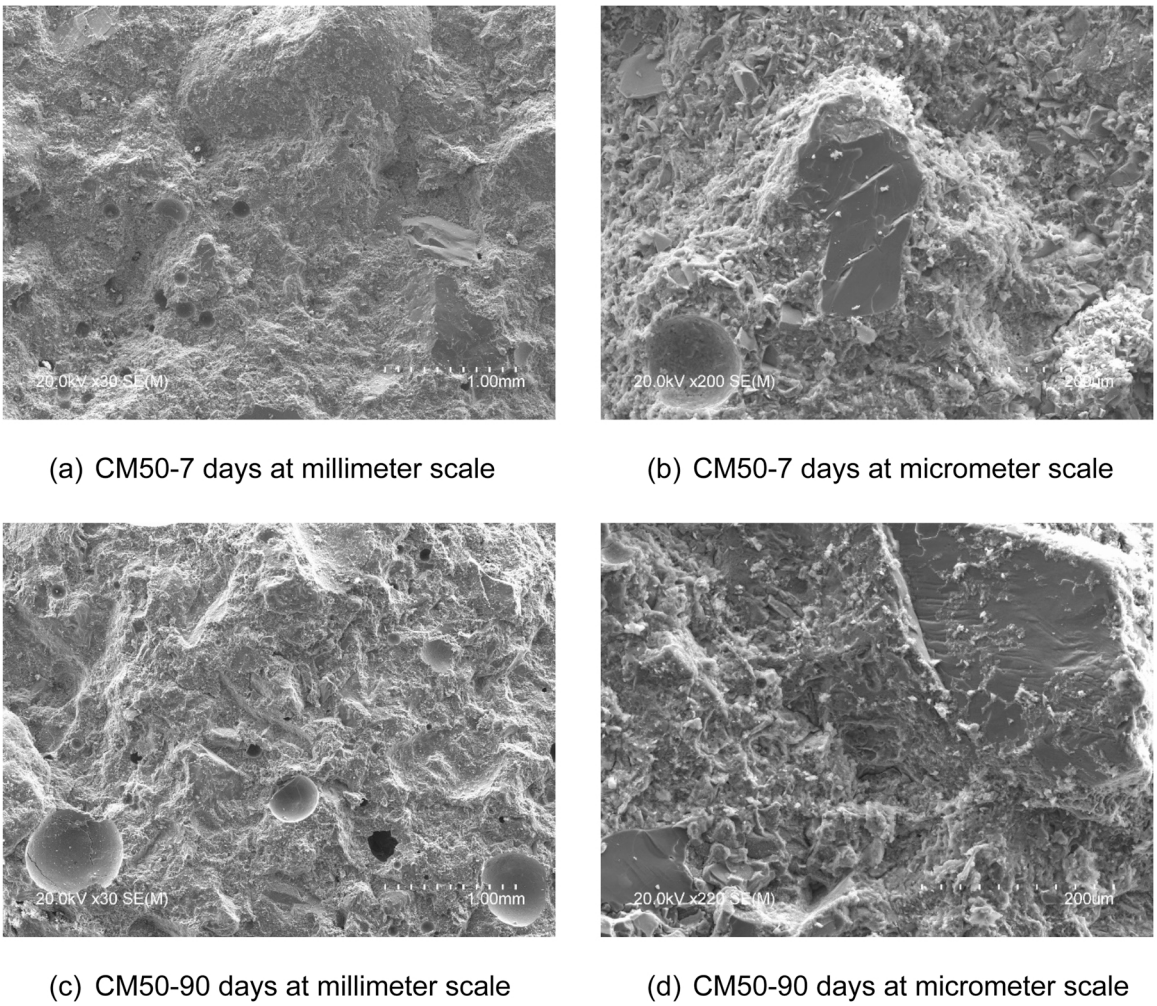

Fig. 8. SEM analysis for CM50 at 7 and 90 days.

the presence of RFA is more frequent and the cement matrix around it is weak being able to be observed in Fig. 9(b). Cracks start from the cement matrix around these RFA and they are interlinked to form failure. The Size of pores is reduced and detachment of RFA is observed in Fig. 9(c). Denser cement matrix with denser hydrated products is formed distance apart from RFA and when it reaches nearer to the recycled fine aggregates the density reduction is observed in Fig. 9(d). The presence of micro-size pores is clearly visible on the surface of the mortar. Smaller particles of RFA contain a greater amount of attached mortar which alters the properties of the new cement matrix in which it is present [71]. The Porosity nature of RFA undoubtedly indicates that the RFA is porous owing to its origin. This porosity eventually leads to (i) lower aggregate specific gravity, (ii) higher water absorption of RFA leading to greater water requirement to maintain an adequate level of workability, (iii) formation of a large total volume of air voids due to their high-volume fraction and (iv) weak binding of aggregate particles in the hardened state [77]. This leads to a reduction in the mechanical properties of mortar with RFA.

The presence of microcracks around the RFA is clearly visible in Fig. 9(d). In previous studies [9,78], the occurrence of cracks within the RFA material happens as a result of the processing activities of RFA. Tam et al., 2015 [79], noted a difference between the microstructures, proposing that RA exhibit two transition zones: one between the original aggregate and the original adhered mortar (the old transition zone) and another between the composite forming the RFA and the new mortar (the new transition zone) [80]. These boundaries have very different features and importantly affect the mechanical behavior of the composites, as the boundary of the new transition zone, tends to have numerous pores and cracks, which reexplains a significant increase in water consumption and compromises the mechanical properties of the materials [21].

The recycled sand is integrated into the cement mass and cannot be distinguished. Only in some of EDS analyzes the potassium content increased slightly, with high silicon content in it. In Fig. 9(b) it can be observed that the C/S is in the range of 2.1–2.8. EDS

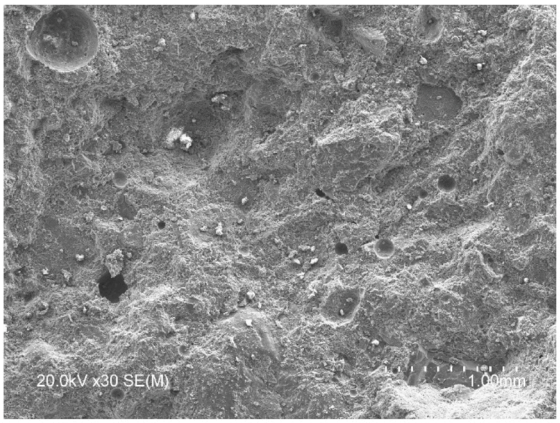

(a) CM100-7 days at millimeter scale

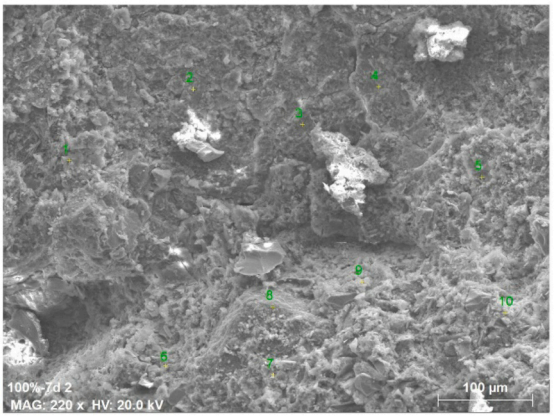

(b) CM100-7 days at micrometer scale

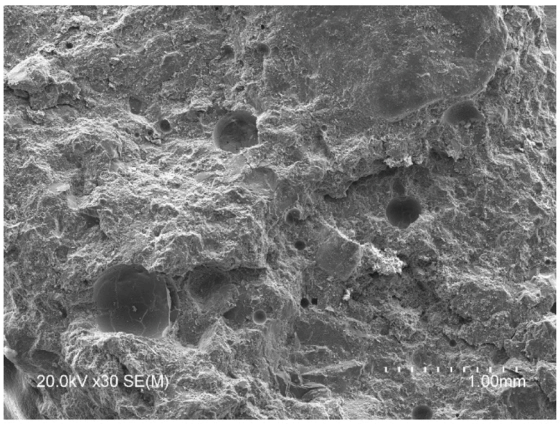

(c) CM100-90 days at millimeter scale

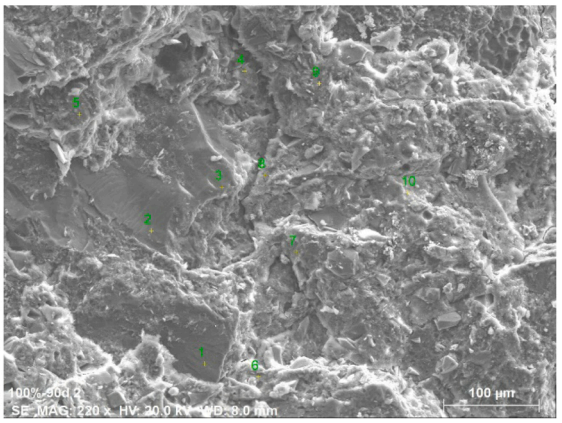

(d) CM100-90 days at micrometer scale

Fig. 9. SEM analysis for CM100 at 7 and 90 days.

analyses as it can be seen in Fig. 9(d), high potassium contents are not observed in any of the samples, although there are points with high contents only of silicon, which could correspond to recycled sand, since there is no standardized sand in this sample. The C/S ratio in hydrated cement is 2.1–2.3.

Different proportions of mineral concentrations present in the recycled mortar at 7 and 90 days are shown in Table 5 and these results are obtained as the average of ten values obtained from ten different locations of sample specimen subjected to EDS. 7 days hydrated CM for C/S is in the range of 2.18–2.30 and it is increased to the range of 2.10–2.85 for 90 days curing period. C/A is 7.07–9.99 for 7 days hydrated sample and it is increased to the range of 10.28–14.70. Whereas the C/F ratio is in the range of 37.39–117.29 for 7 days curing period and it is increased to 44.31–68.76 for 90 days curing period. EDS analyzes carried out on the binder highlight the majority presence of silicon and calcium, a C/Si ratio of 2.10–2.80. Also, there are minor contents of aluminum, sulfur and magnesium. Therefore, as hydration progresses, denser and more compact gels are obtained, with a higher C/S ratio, which could be classified as C-S-H type gels [81]. Lower contents of aluminum, sulfur and magnesium are observed, and to lesser extent potassium.

For the CM25 hydrated sample, the C/S ratio for 7 days is in the range of 1.86–2.75 and it is hydrated much for 90 days curing period as 1.90–2.85. Manzano et al., 2008 [82] noted that the C/S ratio of the CSH increases, aluminum is more likely to be incorporated into pairing tetrahedral position. For well-hydrated cement particles, the C/S ratio in the CSH is variable in the range of 1.2–2.1 [83]. Lower the C/S ratio (in the range of 1.2–2.1) in CSH with an increase in curing time, result in an increase in strength properties [84].

For CM50 hydrated sample, the C/S ratio for 7 days is in the range of 1.99–2.56 and it is much hydrated to 2.09–3.36. There is an increase in the ratio of Ca/Al from 7 days hydrated sample to 90 days hydrated sample. C/A ratio in CM50 hydrated sample is higher than the CM25 hydrated sample. C ratio is observed in the higher ratio for CM50 hydrated sample at 90 days curing period. For CM100 hydrated sample, the C/S ratio for 7 days is in the range of 1.99–2.44 and it is hydrated to 2.08–2.83 for 90 days curing period. C/A ratio is decreased to 5.41–7.61 for 7 days hydrated sample and it is decreased further to 4.73–7.24 for 90 days curing period. Whereas the C/F ratio is decreased for CM100 for 7 days hydrated sample and it is decreased further to 90 days.

CSH gel consists of different phases like C/A, C/S and C/S [85], and the proportions vary for inner and outer CSH. C/S ratio less than 1.5 indicates that the material containing substantial proportions of aggregates [85]. C/A ratio as 2 and C/S ratio as 4 indicates that the presence of monosulfate [85]. C/F ratio as 0 indicates black color in BSE and C/F ratio greater than 50 is observed as gray color and intermediate gray color has the ratio range between 0 and 50 [85]. Outer CSH has a different ratio as observed by Famy et al., 2003 [85] as C/S = 1.9, CaAl = 20 and Ca/S as 12.5. Inner CSH has the different ratio as C/S = 2, C/Al= 16 and C/S = 16. Ca/Si ratio is known to play a key role in the formation of CSH and influences not only the chemistry of the cement matrix but also the properties of the concrete itself [63]. Al/Si ratio in the range of 0–0.14 and Mg/Si is in the range of 0–0.16 for a well-hydrated sample of CSH. The lower C/S ratio has a higher degree of polymerization i.e., it has a crystalline structure and the higher ratio of C/Si has a lower degree of polymerization i.e., has a poor crystalline structure.

Hydrated products in the cement paste matrix are conservatively divided into outer and inner products, defined as products initially formed in space occupied by clinker grain and by water respectively. And the inner product is recognized in the BSE image and it includes clinker grains too small [85]. Both products include CSH and other phases to form CSH gel. Larger bright grains are unreacted products, a mixture of white and gray products is calcium hydroxide and dark color indicates the lower density products like pores observed in Fig. 10. Improper binding of aggregate by hydrated products at initial days is observed in Fig. 10(a) and the cement grains are located away from aggregate which is started to hydrating. Microcracks in the cement paste are clearly visible in Fig. 10(b) indicating that failure takes place initially in cement paste and prolonged towards to ITZ leads to higher mechanical properties. Cement grains which are apart from aggregate are still hydrating as it is observed. The disintegration of small particles in ITZ either from the aggregate particle or from cement grain is noted. Lower mechanical properties of CM25 mortar at 7 days are due to the porous nature of the interface between aggregate and cement paste is observed in Fig. 10(c). Disintegration in unreacted hydrated particles or separation of it is observed indicating that there is no connectivity of pores. In Fig. 10(d), it is observed that there is strong ITZ between aggregate and paste which are light-dark colors. Complete hydration of several cement grain particles which result in small nano-sized pores is noted. Higher mechanical properties of CM25 at 90 days is due to formation of denser CSH between aggregate and cement paste and smaller diameter of pores.

Fig. 10(e) indicates that the pores and some unreacted hydrated particles are noted. Pore sizes at the micro-scale that are randomly scattered. Unreacted cement grains are observed. Whereas in Fig. 10(f) it is observed that the pores are connected and disintegration of

Table 5
Mineral proportions of hydrated cement mortar at 7 and 90 days.

	CM		CM25		CM50		CM100	
	7 Days	90 Days	7 Days	90 Days	7 Days	90 Days	7 Days	90 Days
Ca/Si	2.18–2.30	2.10–2.85	1.86–2.75	1.9–2.85	1.99–2.56	2.09–3.36	1.99–2.44	2.08–2.83
Ca/Mg	8.56–24.93	12.95–46.37	5.23–48.24	5.96–29.47	5.59–25.33	6.12–17.94	5.12–58.81	9.09–11.09
Ca/Fe	37.39–117.29	44.31–68.76	28.62–181.27	28.9–135.95	11.03–125.57	8.49–32.43	18.89–43.87	14.67–25.14
Ca/Na	0–49.85	56.97–284.86	70.38–86.70	0–854.57	0–737.75	0–109.3	58.83–76.07	51.23–67.09
Ca/K	43.99–58.65	51.13–65.02	71.21–72.95	56.97–119.64	19.22–56.75	41.56–128.30	65.57–89.26	69.68–116.04
Ca/S	36.04–38.10	25.78–27.57	35.82–40.15	28.62–40.15	26.12–75.67	22.19–35.13	29.58–46.76	21.24–39.32
Ca/Al	7.07–9.99	10.28–14.70	5.15–13	6.13–10.16	6.25–9.11	7.18–11.46	5.41–7.61	4.73–7.24

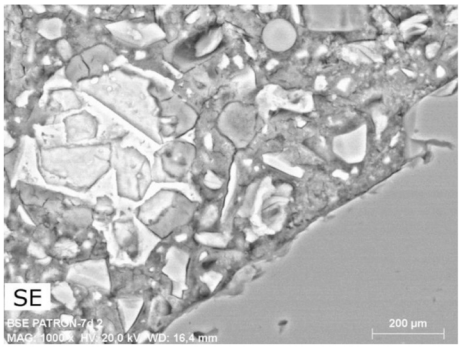

(a) CM at 7 days

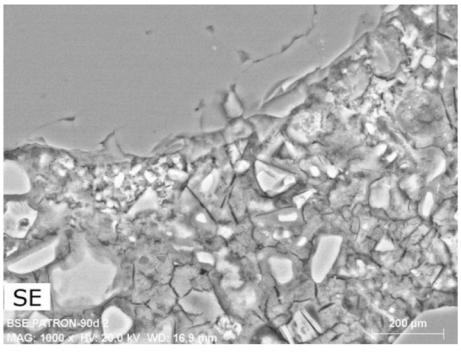

(b) CM at 90 days

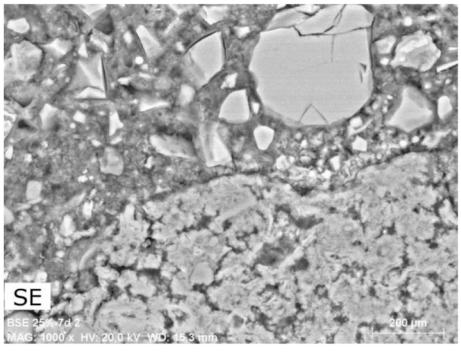

(c) CM25 at 7 days

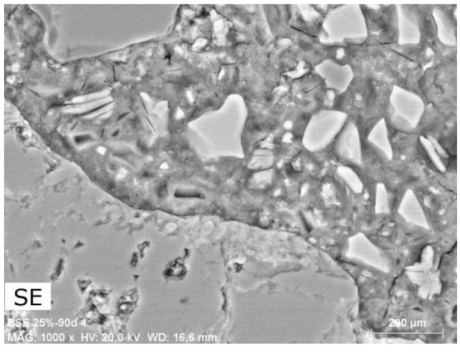

(d) CM25 at 90 days

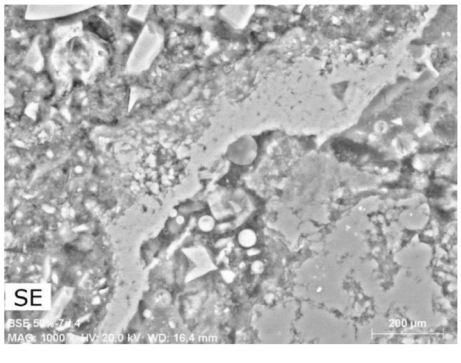

(e) CM50 at 7 days

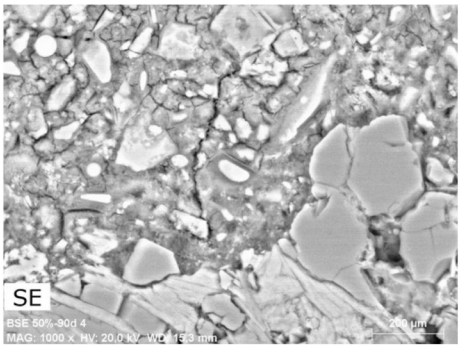

(f) CM50 at 90 days

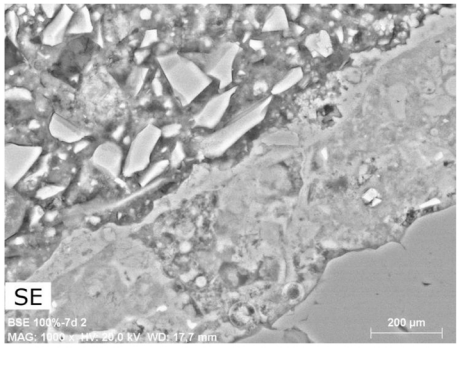

(g) CM100 at 7 days

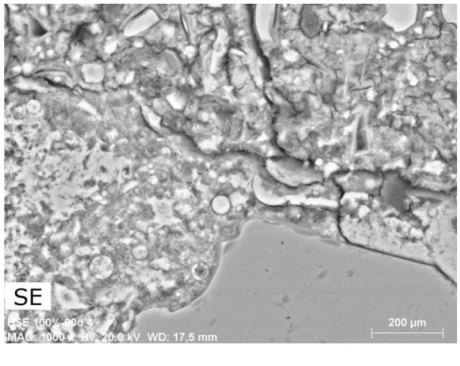

(h) CM100 at 90 days

(caption on next page)

Fig. 10. BSE images of recycled fine aggregate mortar at various curing period.

aggregates at ITZ leads to reduce the load-carrying capacity and this case is further worst in the case of CM100 in Fig. 10(f). Fig. 10(g) clearly shows the presence of old mortar and the cracks propagate through it in the 7- and 90-days curing period.

Comparing various BSE images of the recycled mortar, the identification of alite, belite and portlandite as shown in different phase maps, which coincides quite well with the areas indicated in Fig. 10 as images of gray and white values. Larger pore areas are represented by black areas [84] as observed in Fig. 10(g) and (h). Increase in space between the inner CSH domains with increasing Ca/Si ratio. Lighter gray areas in the BSE micrographs show a higher average atomic number and thereby a higher density considering the resemblance in chemical compositions [84]. Fig. 10(d) and (b) show that the inner CSH areas, despite being well dispersed, are expected to contain few contact points with neighboring inner CSH areas. An increase in such particle association could explain the slightly higher compressive strength for increasing silica contents [84].

In Fig. 11, it is observed that how in control mortar potassium is not present in specific areas, however the use of RFA causes accumulations of potassium in certain areas in the analyzed image, this fact could be due to the presence of ceramic material that accompanies RFA. These ceramic based products usually incorporate potassium feldspars, orthoclase type in their composition.

3.3. Capillary water absorption

Water absorption due to capillary action estimates a larger extent of the durability of mortar because it can seriously influence the exposure of the material to external agents. Governing factor for absorption depends on the structure of the capillary of the material; consequently, the smaller the capillary network, the lower the absorption of mortar. The Durability of cementations materials can be determined indirectly by capillary water absorption [56] and therefore lower water absorption by capillarity indicates more durable rendering mortars when exposed to external environmental agents.

With respect to time, the weight gained by specimens increases with an increase in RFA as observed in Fig. 12 but initially for 45 min, the weight gained remains constant. This is because the initial surface pores occur due to the fact that either excess water present evaporates or due to calcium hydroxide formation as a result of hydration reaction. Weight gained by reference mortar is 5.5% at the end of 1440 min, which is doubled at 100 min and it is the lowest among the mortar mix group. Capillary water absorption coefficient is the lowest (i.e., 0.00011 $kg/m^2.min^{0.5}$) in mortars with the lowest W/C ratio, because it reduced both the space between cement grains and aggregate and the capillary network [86] and increases the adhesion between particles [41]. According to Lenart., 2013 [86] admixtures cause air bubbles to appear and prevent the formation of interconnecting pores, thus interrupting the capillary systems, resulting in reduced capillary water absorption in Fig. 12. But as per Neno et al., 2014 [41], the formation of average pore diameter is reduced due to well defined bridge between cement mortar matrix and aggregates, and also these fine pores are filled by cementations materials result in the lowest capillary rate expressed by the lowest coefficient of capillarity [41] in Fig. 12.

The 25% replacement of NFA by RFA in mortar results in 5.1% weight gain at 360 min, which is increased to 7.1% at 1440 min for CM25 mix. Whereas in the case of CM50, results in 6.1% weight gain at 360 min and it is increased to 8.1% at 1440 min. Water gained is increased slightly due to the increase in average pore diameter, which results in a decrease in the superlative connection between cement matrix and aggregates and probably also due to a decrease in filler effect (presence of a greater number of pores) explaining the increase in capillary rate expressed by the coefficient of capillarity [41] in Fig. 13 which is increased as 0.00015 kg/m^2 $min^{0.5}$ for CM25 mortar mix and 0.00017 $kg/m^2.min^{0.5}$ for CM50 mortar mix compared to reference mix. And another relevant factor is the increase in the amount of free water available in the mix is increased slightly due to the presence of RFA, which leads to an increase in the volume of voids. Water absorption increases with an increase in RFA content in the mix, due to its high-water absorption capacity [86].

Weight gained by CM100 is 8.0% at 360 min and it is increased to 10.7% at 1440 min and it is observed as the highest among the mixed group. Due to the presence of a larger amount of RFA, the water absorption increased because of RFA's high water absorption capacity [86]. However, the water absorption of RFA is lower in the cement matrix when compared to water immersion because the finer particles in the cement matrix fill the pores thereby either reduce the pore size or start further hydration [87]. Characteristics like composition, fineness, surface morphology, texture, and shape play a key role in the water absorption process of the mortar. Differences between the structure of pores in new cement paste and that of recycled aggregates are probably affected by the existence of old cement paste. These parameters may affect the pore connectivity and pore tortuosity in the new cement mortars leading to extensive variation results [88] which is observed in Fig. 13 as higher capillary water absorption coefficient as 0.00024 kg/m^2 $min^{0.5}$. The Capillary water absorption coefficient for CM100 is more than the twice amount of reference mortar is observed and it is due to the complex behavior of RFA. And it is probably a result of using aggregates from recycling plants that treat mixed waste [88]. Capillary absorptions are meaningfully increased in the case of recycled aggregate mortars, due to a greater amount of linked capillary pores [89].

3.4. Water absorption

Water absorption increases with an increase in RFA content as observed in Table 6. These results are coinciding with those observed in the literature [59], [90]. The Higher porous nature of RFA blended mortar with higher RFA content is due to the higher porous of RFA material itself [40]. This is not a significant feature, specifically in outdoor environments, because water is a dangerous agent that has the capacity to damage cementations materials and steel. However, the high open porosity of RFA blended mortars contributes to

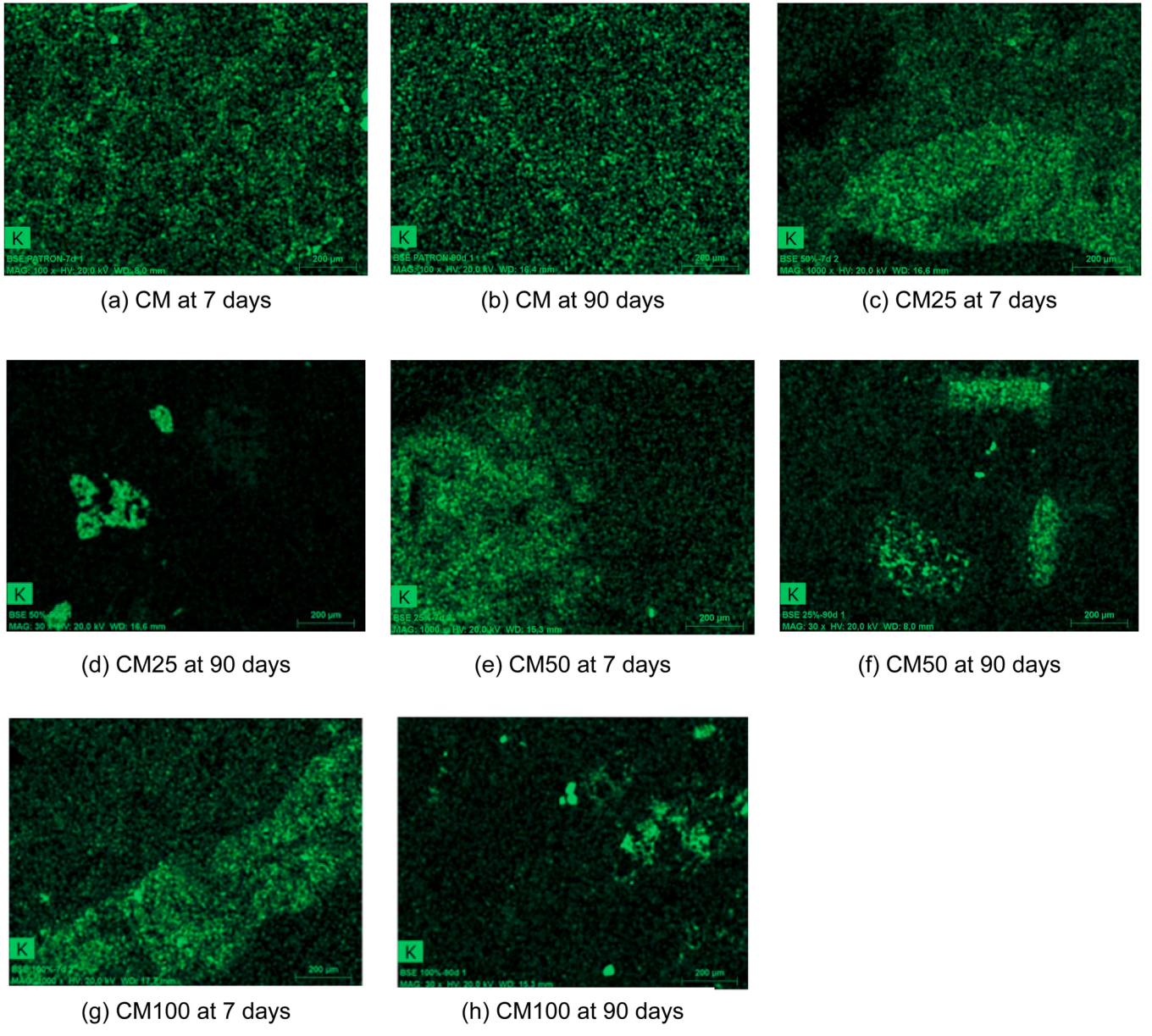

Fig. 11. Concentration of potassium in mortar for various replacement level and at various curing periods.

the better dispersion of CO_2 present in the atmosphere, which over time is valuable to mortar hardened properties and to the environment.

Water absorption of CM25 mortar mix increased 50% more than the reference mortar. When 50% of NFA is replaced by RFA, the water absorption is increased to 97% but when 100% of NFA is replaced by RFA, the water absorption is increased to a highest of 167% than reference mortar is observed in Table 6. But in the case of water immersion vacuum, the absorption values goes double than reference mortar for CM25 and it is increased to 2.7 times for CM50. The highest water absorption value is observed for CM100 which is 4.5 times than reference mortar. Water absorption increases with an increase in RFA content in the mix. It is credited to that the cement mortar adhered to RFA quickens the water uptake and these impacts are increased with an increase in RFA content [1]. For a higher W/C ratio, there are substantial flaws and interconnected pores, as a result of insufficient hydration, enables both uptakes and withheld the water to a substantial level [1].

Dry and apparent density value for control mortar is 2.236 and 2.406. There is a reduction of about 4.5% of dry density and an increase of about 5.3% of apparent density for CM25 than control mortar is observed. In the case of CM50, the dry density is decreased to 6.2% and apparent density is increased to 6% than control mortar. The highest change in density is observed for CM100 with a reduction of about 11.5% for dry density and an increase of about 14.1% than control mortar is observed. The dry density of the mortar in a hardened state was observed to decrease with an increase in RFA content as observed from previous studies [21], [78]. This is because the bulk density of RFA itself is lower than the NFA. Fig. 14, shows the comparison for the density of mortar at various curing periods to the dry density, apparent density and porosity of mortar with RFA.

Permeable void content for control mortar is 7.075 and when partial replacement of NFA by RFA is increased to 25%, the porosity is increased to 15.735. It is observed that the permeable void content value is increased twice for CM25 than the control mortar mix. Partial replacement of NFA by RFA is increased further to 50%, the Permeable void content is increased further to 17.753 but when the replacement percentage is increased to 100%, the permeable void content is increased four times approximately i.e., 27.920. A common observation that, with an increase in RFA content, permeable voids are increased and it is also reported in previous studies [1] and it is due to the following two reasons. First, the surface morphology of RFA is porous in nature, and secondly, surface area of RFA is large. Hence, an increase in RFA content results in an increase in W/C ratio and on hardening process, this excess water evaporates and creates more pores in paste volume.

3.5. Porosity

In Fig. 15(a), it is observed that with an increase in the curing period there is a decrease in total porosity and pore size for all mortars is observed. For 7 days curing period, the total porosity for the control mortar is 12.056%, it is increased to 14.349% for CM25, it is further increased to 17.762% for CM50 and it is increased to 20.671% for CM100. With the increase in the recycled aggregate, there is an increase in the percentage of total porosity is observed. For 90 days curing period, the total porosity for control mortar is 8.984%, it is increased to 12.917% for CM25, for CM50 it is increased to 13.508% and for CM100 it is increased further to 16.417%. Porosity increases with an increase in RFA content are observed in previous studies [28] irrespective of curing periods. A Decrease in total porosity for control mortar is observed as 3.072 and for CM25 it is observed as 1.432 for 7 days to 28 days curing period and also, for CM50 and CM100 it is observed that 4.254. The total porosity of mortar contains RFA has a higher porosity than the control mix and it is also observed by García-Gónzalez, et al., 2015 [91].

This is due to high pores in the old paste and the porous nature of RFA itself. On increase in curing period, there is a decrease in total porosity is observed due to the formation of more hydration products which will occupy the pores. Several studies state that a higher porosity of components results in poor performance in both strength and durability properties [91], [92]. It is stated in the literature that the critical pore diameter of the capillary pores varies from 10 nm to 10,000 nm [93]. By means of water in pores of RFA, a water movement between the new cement paste and the RFA is created, moisture contained in the pores of the paste are slowly released to allow continuous hydration, which leads to the refinement of pore structure [28].

Increase in content of RFA result in a decrease in means of the diameter of pores is observed in Fig. 15(b). The Mean pore diameter for control mortar is observed as 0.0306 μm for 7 days curing period, pore diameter size is decreased to 0.0278 μm for CM25, it is

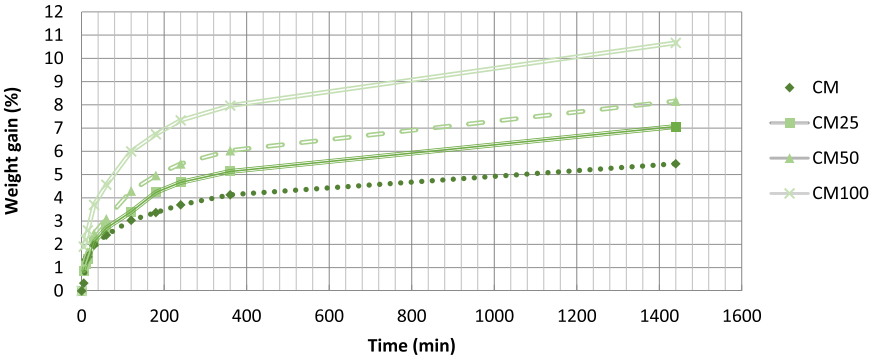

Fig. 12. Water absorption by capillarity of the mortar samples.

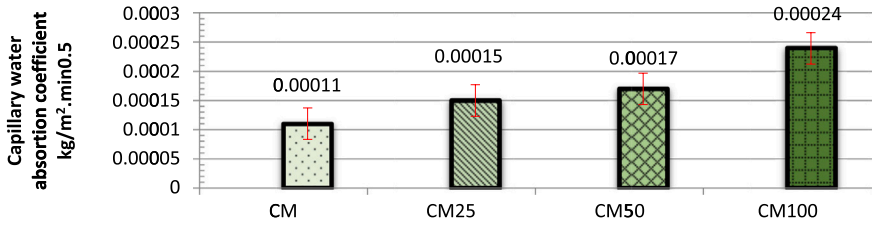

Fig. 13. Average water absorption coefficient by capillarity of the mortar samples.

decreased to 0.0253 μm for CM50 and it decreased further to 0.0225 μm for CM100. At 7 days curing period, with an increase in RFA content, the average pore size increases and it is in the range of 0.0306–0.0225 μm is noted. The Reason for the increase in the average size of pores is 1. Old cement paste adhered to RFA content is porous in nature, 2. the new paste formed to attach the RFA and cement matrix is a week in nature, 3. RFA itself has pores 4. Higher W/C ratio. The mean pore diameter is increased for 90 days curing period, as it is well observed that with an increase in curing period there is more formation of hydration products. The mean pore diameter for control mortar at 90 days curing period is increased to 0.0141 μm, it is decreased to 0.0174 μm for CM25, mean pore diameter is increased to 0.0154 μm for CM50 and it is increased further to 0.0151 μm. With the increase in the percentage of RFA, there is the formation of more amount of hydration products up-to a certain level and after that there is presence of RFA in system itself creates more pores.

Pore size distribution of RFA mortar is widened and shifts to lower pore size with an increase in replacement of NFA by RFA as observed in Fig. 15(a). As already discussed, there are so many reasons for the formation of different sizes of pores in CM100. On reduction of RFA content to 50%, i.e., CM50 mortar, the distribution of pore size reduced as content of RFA is decreased. And on further reduction to 25%, i.e., CM25 mortar, the distribution of pore size is reduced further, and curve becoming narrow is observed. Finally, for controlled mortar, the curve becomes narrowed indicating that the size of pores distributed is even. A decrease in pores size distribution for all mortar mixes for an increase in curing period to 90 days is observed in Fig. 15(b). When compared to 7 days curing period, CM100 for 90 days is narrowed due to more formation of hydration products. On decreasing the RFA content to 50% substitution for NFA, the distribution curve is decreased along with a decrease in pore size. But when 25% of NFA is substituted by RFA, the pore size distribution is even and narrowed than reference mortar and this is the reason for improved mechanical and durability properties. Hydration products formed are evenly distributed and the size of pores is reduced evenly.

Reference mortar possesses the narrow distribution of pores for 7 days and it is decreased for 90 days curing period. For CM25 mortar mix, the distribution of pores is even and finer pores are found more for both 7- and 90-days curing period. When RFA content is increased to 50%, the pores increased and the distribution of pores is also increased which result in the widening of the distribution of the curve for 7 days curing period and it is slightly narrowed in the case of 90 days curing period. When NFA is replaced by RFA about 100%, at 7 days curing period, pore size is increased and also the distribution of pores is increased further which result in widening of distribution curve.

But for 90 days curing period, the pore size is decreased and the distribution of different pore sizes are also decreased which result in a decrease of the widened distribution curve as noted from Fig. 16(b). At 7 days curing period, the maximum pore size is available in between 0.1 and 0.01 μm as shown in Fig. 16(a) and next to it is 1–0.1 μm pores are available as highest in all the mix. CM100 consists of highest proportion of these two pores hence it produces lesser strength characteristics. Due to presence of old adhered mortar in mix and improper binding of RFA to cement matrix results in larger proportion of capillary pores. Quantity of these two pores is reduced with a decrease in RFA content is observed. Formation of more amount of macro pores result in a decrease in properties of mortar at 7 days, whereas the formation of micro pores is very less.

With an increase in curing period, the formation of hydration products increases result in a decrease in pores as observed when Fig. 17(a) and 17(b) are compared. Reduction in the formation of macro pores is observed in the all-replacement. This is due to formation of hydration products which will occupy the macro pores thereby refining the pore size distribution and reducing the size of pores [94]. Quantity of pores of size less than 0.1 μm has been shown to have a less negative effect on the mechanical and durability properties [36], [95] and these pores are related to CSH phases. Pore size greater than 0.1 μm is related in interparticle pores and these pores related to the capillary moment of water in between particles. There is much change in these capillary moments and it is related to pores as observed with respect to RFA content for various curing period. Increase in the micro pore content for the mix CM25 which is similar to that of a standard mix is observed. But for other mixes, the micro pore proportion is very less due to non-availability of any required minerals for hydration reaction or larger amount of adhered old mortar.

Table 6
Absorption values after immersion, absorption after immersion and vacuum, dry density, apparent density and permeable voids accessible to water.

	Absorption di.	Absorption iv	Dry density	Ap. Density	Permeable voids
CM	3.164	3.164	2.236	2.406	7.075
CM25	4.746	7.368	2.135	2.534	15.735
CM50	6.222	8.459	2.098	2.551	17.753
CM100	8.355	14.108	1.979	2.745	27.920

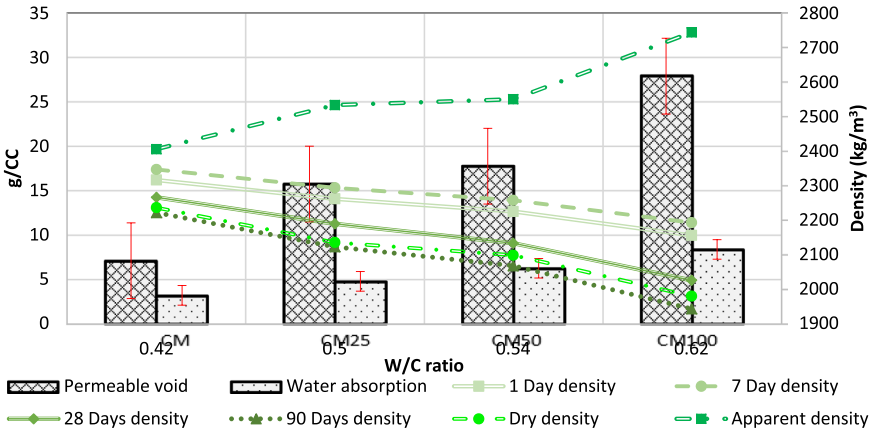

Fig. 14. Compared values of absorption after immersion, absorption after immersion and vacuum, dry density, apparent density and permeable void content to actual density.

3.6. Effect of pore size on strength

Porosity can affect the strength parameters of mortar as already studied by Hu et al., 2019 [96] and Shi et al., 1989 [97]. In Fig. 18, it is observed that the pore size and pore size distribution of recycled aggregate mortar is the function of mechanical properties. Fig. 18 (a) and 18(c) indicate that the decrease in particle size less than 1 μm with an increase in replacement of NFA results in decreases in strength. Combination of pore sizes between 1 μm and 0.01 μm is in higher proportion results in lower mechanical properties. And this may due to higher W/C ratio result in formation of more macro pores and also due to presence of old mortar adhering to RFA. In Fig. 18 (b) and 18(d), it is observed that the higher compressive strength for the mixture having lesser percentage of particles less than 1 μm. This may due to hydration reaction take place inside the macro pores which are present during initial days. When calcium hydroxide leaches out to reach silica or aluminum minerals, leading to further hydration reaction and refining the pore structure thereby reducing the diameter of pores. Hence, the mix becomes more homogenous and denser in nature, contributing to the improved mechanical and durability properties.

Similar results are reported by Hu et al., 2019 [96] as decreasing in smaller pores results in increasing in compressive strength. From this, it can be understood that the strength of mortar is an essential function of pore form, pore size distribution and porosity [98] within it and irrespective of curing period. Strength is primarily influenced by pore size distribution rather than average pore volume [98]. In Fig. 18, it is also observed at early ages of mortar, the governing factor for strength is pore size while at later ages, porosity becoming controlling factor. Two different types of pores are reported by Kendall et al., 1983 [98]. Gel pores which are located within cement matrix gel are too small to initiate crack when loading and capillary pores which occur as a result of hydration of cementitious materials are higher in dimension and easily initiate cracking while loading [98]. Threshold radius for gel pore in cementitious gel is reported as 0.1 μm as reported by O'Farrell et al., 2001 [94] but in this study, the threshold radius for gel pore is observed as 1 μm.

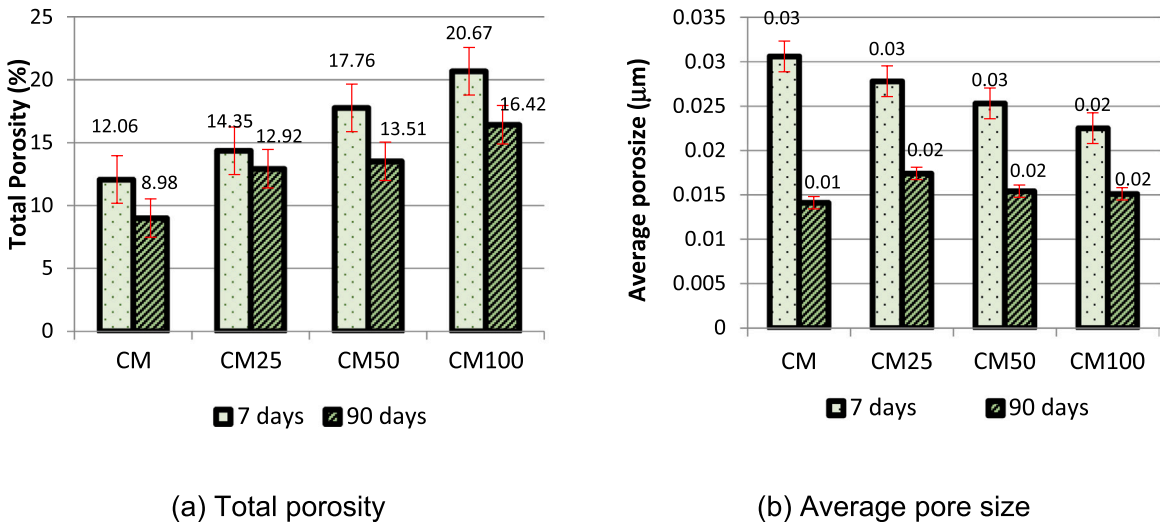

Fig. 15. Porosity of recycled aggregate mortar.

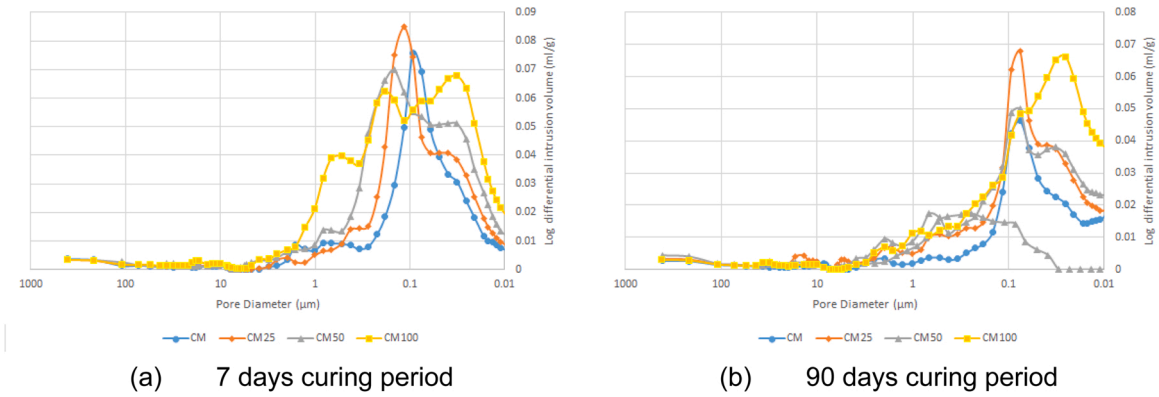

Fig. 16. Pore size distribution of recycled aggregate mortar with respect to different curing period.

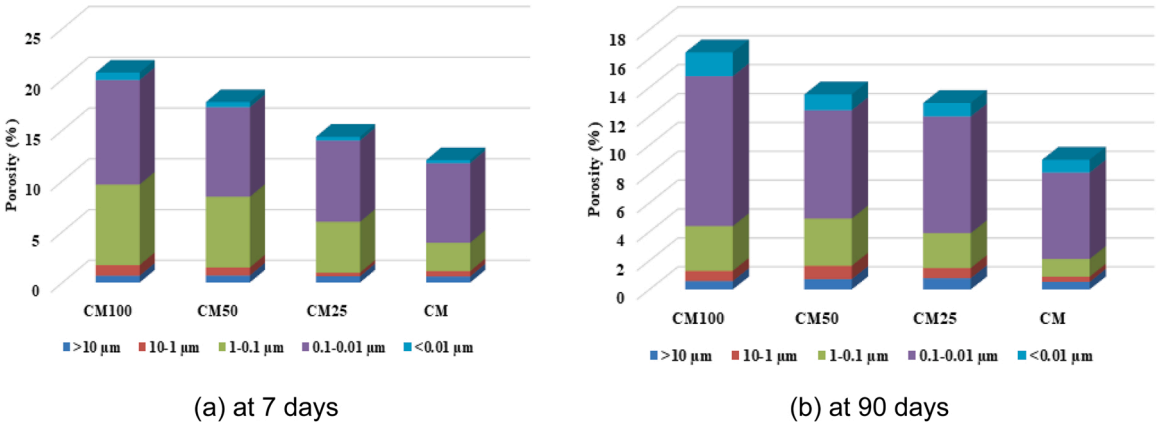

Fig. 17. Pore size distribution among different replacement of recycled aggregate.

Threshold radius is defined as the radius of pore at which there is a sudden increase in pore radius and thereby an increase in the cumulative volume of pores [94]. In Fig. 18, it can be observed that the threshold radius is the function of W/C ratio of mix and increase in the W/C result in increase in threshold radius [94]. Another notable observation made is that the higher strength characteristics is a function of pore size and size distribution of pores. When relative humidity of capillary pores is maintained above 80%, which will make possible environment for hydration reaction [99].

3.7. Relationship between strength and porosity

Limited literature is available in the relationships between strength and porosity of engineering materials. Hence, the validate above discussion few relationships are available in literature. Relationship between compressive strength (f_{cm}), compressive strength at zero porosity (f_{cm0}) and POR was suggested by Balshin, 1949 [100] as:

$$f_{cmt} = f_{cmt0}[1 - POR]^{b} \tag{2}$$

Compressive strength (f_{cmk}), compressive strength at zero porosity (f_{cmk0}) and POR relationship was suggested by Ryshkewitch [101] as:

$$f_{cmk} = f_{cmk0}\ e^{-KPOR} \tag{3}$$

Generally, strength (f_{cm}), zero porosity (P_0) and POR relationship were suggested by Schiller [102] as:

$$f_{cm} = n\log\left[\frac{P_o}{POR}\right] \tag{4}$$

Linear relationship between f_{cm}, strength at zero porosity (f_{cm0}) and POR was suggested by Hasselman [103] as:

$$f_{cm} = f_{cm0} - c\ POR \tag{5}$$

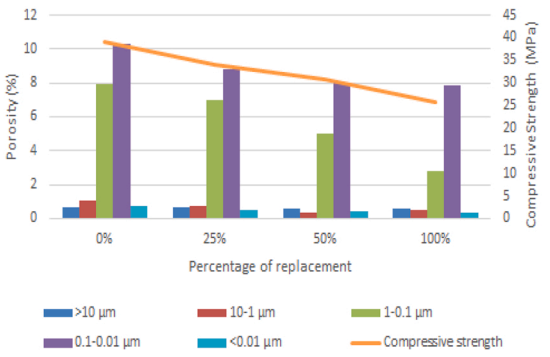

(a) Compressive strength and pore size at 7 days for various percentage of replacement.

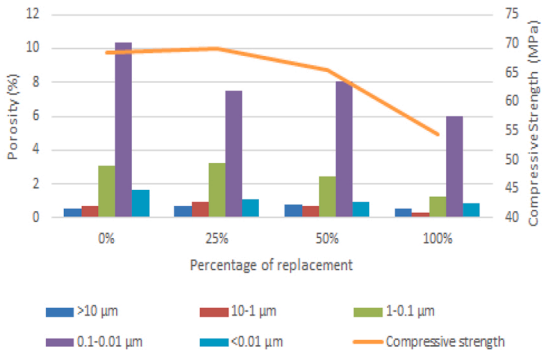

(b) Compressive strength and pore size at 90 days for various percentage of replacement.

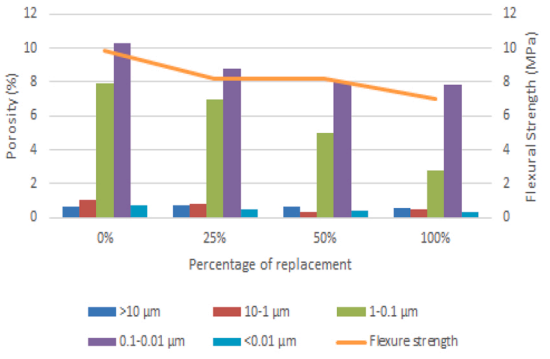

(c) Flexural strength and pore size at 7 days for various percentage of replacement.

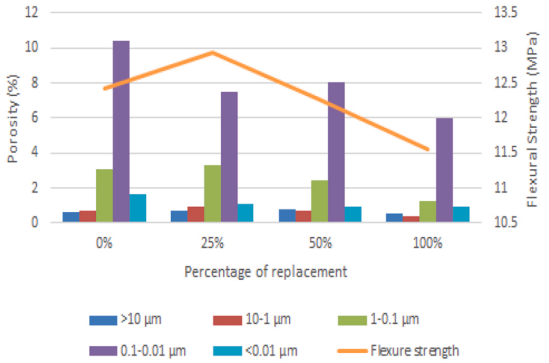

(d) Flexural strength and pore size at 90 days for various percentage of replacement.

Fig. 18. Strength and pore size at 7 and 90 days for various percentage of replacement.

Where, b, k, n and c are empirical constants.

Constant's 'b', 'k', 'P_0' and 'c' are said to be dependent constants. These constants depend on the value of POR. Constant 'f_{cmt0}', 'f_{cmk0}', 'f_{cm0}' and 'f_{cm0}' are independent constants which didn't depend upon any factors. Constants for these relationships are determined from the general fit statistical equations and it is reported in Table 7.

Which can be determined from general fit statistical equations.

In Fig. 19(a), it is observed that the equation proposed by Balshin., 1959 [100] makes more appropriate prediction in the relationship between compressive strength and porosity at 7 days. Whereas, the compressive strength predicted by Ryshketwitch., 1953 [101] and Schiller., 1971 [102] overestimates the strength during initial porosity stage. But the equation proposed by Hasslemen., 1962 [103] underestimates the strength. But in the case of 90 days curing period, the equation proposed by Schiller., 1971 [102] overestimating at initial and at later porosity stage as observed in Fig. 19(b). Equations proposed to other researchers are similar in nature is observed. With respect to the flexural strength of RFA blended mortar, similar trend to that of compressive strength is observed for both 7- and 90-days curing period is observed in Fig. 19 (c) and 19(d).

Table 7
Constants for relationship between the strength and porosity at 7 and 90 days.

Constants		f_{cmt0}	B	f_{cmk0}	k	P_0	n	f_{cm0}	c
Compressive strength	7 days	63.05	3.811	67.095	-4.559	1	23.269	55.971	-145.36
	90 days	91.727	2.574	93.524	-2.915	1	20.117	87.577	-178.59
Flexural strength	7 days	13.698	2.84	14.359	-3.402	1	4.582	12.931	-28.369
	90 days	13.748	0.809	13.821	-0.91	1	1.165	13.708	-10.917

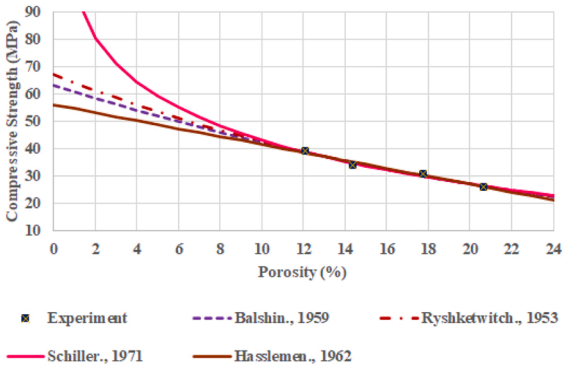

(a) Porosity Vs compressive strength at 7 days.

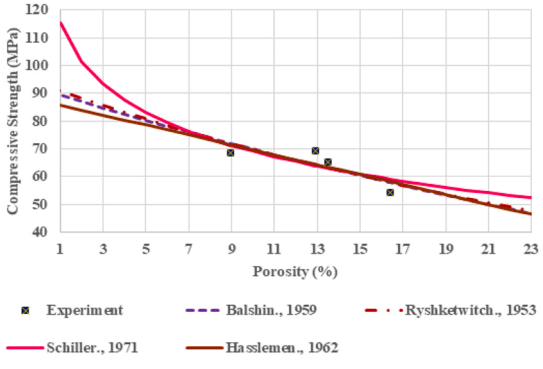

(b) Porosity Vs compressive strength at 90 days.

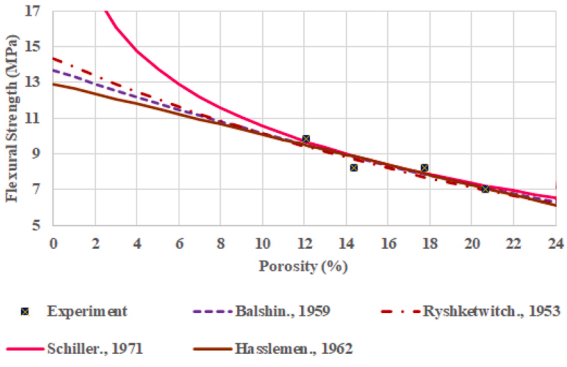

(c) Porosity Vs flexural strength at 7 days.

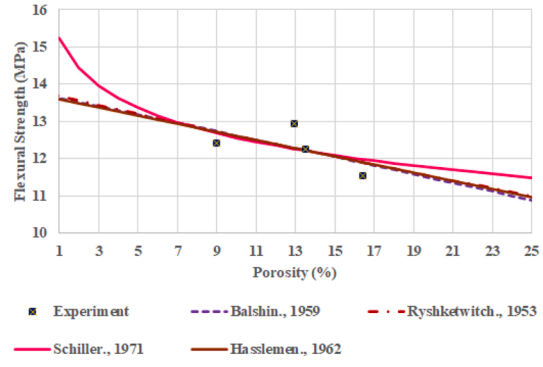

(d) Porosity Vs flexural strength at 90 days.

Fig. 19. Porosity vs strength with respect to various models in literatures, experiment and at different curing periods.

4. Conclusions

This paper presents an experimental investigation on the influence of partial replacement of NFA by RFA on hardened properties of mortar. Hardened properties including mechanical properties and water- related durability studies. The following conclusions were drawn:

- W/C ratio increases with an increase in RFA content due to increased surface area of RFA and its irregular shape with porous in it. Real density decrease linearly as the replacement ratio of natural sand by RFA increases, due to the lower density of RFA.
- Compressive and flexural strength decreases with an increase in RFA content in the mix for initial curing periods but on a longer curing period, the CM25 mortar strength reaches the value of control mix value. C/S ratio in the hydrated pastes lies between 1.9 and 2.8 for all the mortar cases and slightly higher for CM25 mortar.Different sizes of pores, hydration products, growth of crack and differentiation of RFA in the hardened state is observed using SEM. BSE shows the ITZ formation between aggregate and cement matrix. Formation of hydrated and unhydrated compounds are clearly noted. In the mapping carried out by means of BSE, it is highlighted that with the incorporation of RFA, there are accumulations of potassium, possibly from felspars present in ceramic products.
- Due to the high absorption of RFA, an important reduction of the workability period is observed in RFA blended mortars. Because of this characteristic absorption by a capillarity increase is also observed. An increase in RFA content decreases the dry density and increases the permeable void content in mortar mix. This is due to the water absorption feature of RFA and the surface morphology of RFA itself.
- An increase in total porosity content with an increase in RFA content in mortar is observed. For CM25, the distribution of pores is narrowed for a longer curing period which fills the voids and increases the mechanical performance when compared to all other mixes. It is observed that the decrease in micro and macro pores results in an increase in mechanical properties. Pore size, pore volume and pore size distribution of pores is becoming fundamental function of mechanical properties. Relationship between porosity and strength satisfies the equations proposed by researchers in literatures during longer curing period.

From the results of this study, the use of FRA is recommended for a longer period of usage at a replacement level of 25% in order to achieve the sustainability in the construction sector.

Conflict of Interest

Authors do not have any conflict of interest.

Data Availability

There are no data availability with this article.

Acknowledgements

Author wish to thank for the supports and guidance given by faculties from University of Leon, Leon, Spain and Coimbatore Institute of Technology, Coimbatore, India.

References

[1] G. Santha Kumar, Influence of fluidity on mechanical and permeation performances of recycled aggregate mortar, Constr. Build. Mater. 213 (2019) 404–412, https://doi.org/10.1016/j.conbuildmat.2019.04.093.
[2] S. Roque, C.M. Pederneiras, C.B. Farinha, J. de Brito, R. Veiga, Concrete-based and mixed waste aggregates in rendering mortars, in: Materials, 13, 2020, p. 1976, https://doi.org/10.3390/MA13081976.
[3] M. Amin, A.M. Zeyad, B.A. Tayeh, I. Saad Agwa, Effects of nano cotton stalk and palm leaf ashes on ultrahigh-performance concrete properties incorporating recycled concrete aggregates, Constr. Build. Mater. 302 (July) (2021), 124196, https://doi.org/10.1016/j.conbuildmat.2021.124196.
[4] M. Amin, B.A. Tayeh, I.S. Agwa, Effect of using mineral admixtures and ceramic wastes as coarse aggregates on properties of ultrahigh-performance concrete, J. Clean. Prod. 273 (2020), 123073, https://doi.org/10.1016/j.jclepro.2020.123073.
[5] M. Amin, A.M. Zeyad, B.A. Tayeh, I. Saad Agwa, Engineering properties of self-cured normal and high strength concrete produced using polyethylene glycol and porous ceramic waste as coarse aggregate, Constr. Build. Mater. 299 (March) (2021), 124243, https://doi.org/10.1016/j.conbuildmat.2021.124243.
[6] Commission, E. , EU Construction & Demolition Waste Management Protocol, 2016.
[7] Commission, E. , Guidelines for the Waste Audits before Demolition and Renovation Works of Buildings, 2018.
[8] G.M. Cuenca-Moyano, J. Martín-Pascual, M. Martín-Morales, I. Valverde-Palacios, M. Zamorano, Effects of water to cement ratio, recycled fine aggregate and air entraining/plasticizer admixture on masonry mortar properties, Constr. Build. Mater. 230 (2020), 116929, https://doi.org/10.1016/J.CONBUILDMAT.2019.116929.
[9] M. Etxeberria, E. Vázquez, A. Marí, M. Barra, Influence of amount of recycled coarse aggregates and production process on properties of recycled aggregate concrete, Cem. Concr. Res. 37 (5) (2007) 735–742, https://doi.org/10.1016/j.cemconres.2007.02.002.
[10] L. Evangelista, M. Guedes, J. De Brito, A.C. Ferro, M.F. Pereira, Physical, chemical and mineralogical properties of fine recycled aggregates made from concrete waste, Constr. Build. Mater. 86 (2015) 178–188, https://doi.org/10.1016/j.conbuildmat.2015.03.112.
[11] Zhao, Z.; Remond, S.; Damidot, D.; Courard, L. , UNE Nouvelle Méthode de Caractérisation des Granulats Recyclés Industriels: Application Aux, in Proceedings of th Conférence Internationale Francophone NoMaD, 2015, 1–12.
[12] Z. Zhao, S. Remond, D. Damidot, W. Xu, Influence of fine recycled concrete aggregates on the properties of mortars, Constr. Build. Mater. 81 (2015) 179–186, https://doi.org/10.1016/j.conbuildmat.2015.02.037.
[13] A. Adesina, A.R. de Azevedo, M. Amin, M. Hadzima-Nyarko, I.S. Agwa, A.M. Zeyad, B.A. Tayeh, Fresh and mechanical properties overview of alkali-activated materials made with glass powder as precursor, Clean. Mater. 3 (2022), 100036, https://doi.org/10.1016/j.clema.2021.100036.
[14] M. Abed, R. Nemes, B.A. Tayeh, Properties of self-compacting high-strength concrete containing multiple use of recycled aggregate, J. King Saud. Univ. Eng. Sci. 32 (2) (2020) 108–114, https://doi.org/10.1016/j.jksues.2018.12.002.
[15] C.S. Poon, Z.H. Shui, L. Lam, Effect of microstructure of ITZ on compressive strength of concrete prepared with recycled aggregates, Constr. Build. Mater. 18 (6) (2004) 461–468, https://doi.org/10.1016/j.conbuildmat.2004.03.005.
[16] G. Bonifazi, R. Palmieri, S. Serranti, Evaluation of attached mortar on recycled concrete aggregates by hyperspectral imaging, Constr. Build. Mater. 169 (2018) 835–842, https://doi.org/10.1016/J.CONBUILDMAT.2018.03.048.
[17] A. Djerbi Tegguer, Determining the water absorption of recycled aggregates utilizing hydrostatic weighing approach, Constr. Build. Mater. 27 (1) (2012) 112–116, https://doi.org/10.1016/j.conbuildmat.2011.08.018.
[18] J.R. del Viso, J.R. Carmona, G. Ruiz, Shape and size effects on the compressive strength of high-strength concrete, Cem. Concr. Res. 38 (3) (2008) 386–395, https://doi.org/10.1016/j.cemconres.2007.09.020.
[19] Z. Li, J. Liu, J. Xiao, P. Zhong, A method to determine water absorption of recycled fine aggregate in paste for design and quality control of fresh mortar, Constr. Build. Mater. 197 (2019) 30–41, https://doi.org/10.1016/J.CONBUILDMAT.2018.11.115.
[20] C.S. Poon, Z.H. Shui, L. Lam, H. Fok, S.C. Kou, Influence of moisture states of natural and recycled aggregates on the slump and compressive strength of concrete, Cem. Concr. Res. 34 (1) (2004) 31–36, https://doi.org/10.1016/S0008-8846(03)00186-8.
[21] J.J. de Oliveira Andrade, E. Possan, J.Z. Squiavon, T.L.P. Ortolan, Evaluation of mechanical properties and carbonation of mortars produced with construction and demolition waste, Constr. Build. Mater. 161 (2018) 70–83, https://doi.org/10.1016/J.CONBUILDMAT.2017.11.089&QID=2&DOC=53&RECORDID=&COLNAME=WOS.
[22] J. Silva, J. de Brito, R. Veiga, Recycled red-clay ceramic construction and demolition waste for mortars production, J. Mater. Civ. Eng. 22 (3) (2010) 236–244, https://doi.org/10.1061/(asce)0899-1561(2010)22:3(236).
[23] Leite, M.B.; Gualberto Figueirêdo Filho, J.L.; L Lima, P.R.; Leite, M.B.; G L Figueirêdo Filho Á P R L Lima, Á.J.; L Figueirêdo Filho, J.G.; L Lima, P.R., Leite Á P R L Lima PPGECEA, M. B., Transnordestina, A., Horizonte, n-N. Erratum: Workability study of concretes made with recycled mortar aggregate (materials and structures, (2013), 46 (10), (1765–1778); Materials and Structures/Materiaux et Constructions. Springer Netherlands October 1, 2013, 1779. ⟨https://doi.org/10.1617/S11527-012-0010-4⟩; ⟨https://doi.org/10.1617/s11527–013-0024–6⟩.
[24] F. Agrela, M. Sánchez De Juan, J. Ayuso, V.L. Geraldes, J.R. Jiménez, Limiting properties in the characterisation of mixed recycled aggregates for use in the manufacture of concrete, Constr. Build. Mater. 25 (10) (2011) 3950–3955, https://doi.org/10.1016/j.conbuildmat.2011.04.027.
[25] Mir, A. El; Nehme, S.G.; Nehm, K. , Építôanyag § Journal of Silicate Based and Composite Materials. ⟨https://doi.org/10.14382/epitoanyag-jsbcm.2015.18⟩.
[26] E.T. Dawood, M. Ramli, High strength characteristics of cement mortar reinforced with hybrid fibres, Constr. Build. Mater. 25 (5) (2011) 2240–2247, https://doi.org/10.1016/J.CONBUILDMAT.2010.11.008.
[27] M.J. Chinchillas-Chinchillas, M.J. Pellegrini-Cervantes, A. Castro-Beltrán, M. Rodríguez-Rodríguez, V.M. Orozco-Carmona, H.J. Peinado-Guevara, Properties of mortar with recycled aggregates, and polyacrylonitrile microfibers synthesized by electrospinning, Mater 12 (23) (2019) 3849, https://doi.org/10.3390/MA12233849.

[28] K. Zitouni, A. Djerbi, A. Mebrouki, Study on the microstructure of the new paste of recycled aggregate self-compacting concrete, Materials 13 (9) (2020), https://doi.org/10.3390/ma13092114.
[29] R. Kumar, B. Bhattacharjee, Porosity, pore size distribution and in situ strength of concrete, Cem. Concr. Res. 33 (1) (2003) 155–164, https://doi.org/10.1016/S0008-8846(02)00942-0.
[30] Q. Zeng, K. Li, T. Fen-Chong, P. Dangla, Analysis of pore structure, contact angle and pore entrapment of blended cement pastes from mercury porosimetry data, Cem. Concr. Compos. 34 (9) (2012) 1053–1060, https://doi.org/10.1016/j.cemconcomp.2012.06.005.
[31] Y.C. Choi, J. Kim, S. Choi, Mercury intrusion porosimetry characterization of micropore structures of high-strength cement pastes incorporating high volume ground granulated blast-furnace slag, Constr. Build. Mater. 137 (2017) 96–103, https://doi.org/10.1016/j.conbuildmat.2017.01.076.
[32] F. Moro, H. Böhni, Ink-Bottle Effect in Mercury Intrusion Porosimetry of Cement-Based Materials, 246, Elsevier, 2002, https://doi.org/10.1006/jcis.2001.7962.
[33] S. Kou, C.S. Poon, Compressive strength, pore size distribution and chloride-ion penetration of recycled aggregate concrete incorporating class-F fly ash, J. Wuhan. Univ. Technol. Mater. Sci. Ed. 21 (4) (2006) 130–136, https://doi.org/10.1007/BF02841223.
[34] Uchikawa, H.; Hanehara, S. , Concrete for environment enhancement and protection: proceedings of the international conference held at the University of Dundee, Scotland, UK on 24–26 June 1996, (Libro, 1996) ⟨https://www.worldcat.org/title/concrete-for-environment-enhancement-and-protection-proceedings-of-the-international-conference-held-at-the-university-of-dundee-scotland-uk-on-24–26-june-1996/oclc/35235723⟩ (Accessed 20 May 2021).
[35] J.M.V. Gómez-Soberón, Porosity of recycled concrete with substitution of recycled concrete aggregate: an experimental study, Cem. Concr. Res. 32 (8) (2002) 1301–1311, https://doi.org/10.1016/S0008-8846(02)00795-0.
[36] Gómez Soberón, J.M. V. , Relationship Between Gas Adsorption and the Shrinkage and Creep of Recycled Aggregate Concrete, 2003.
[37] J.M. Khatib, Properties of concrete incorporating fine recycled aggregate, Cem. Concr. Res. 35 (4) (2005) 763–769, https://doi.org/10.1016/j.cemconres.2004.06.017.
[38] S.C. Kou, C.S. Poon, Properties of concrete prepared with crushed fine stone, furnace bottom ash and fine recycled aggregate as fine aggregates, Constr. Build. Mater. 23 (8) (2009) 2877–2886, https://doi.org/10.1016/j.conbuildmat.2009.02.009.
[39] L. Evangelista, J. de Brito, Mechanical behaviour of concrete made with fine recycled concrete aggregates, Cem. Concr. Compos. 29 (5) (2007) 397–401, https://doi.org/10.1016/j.cemconcomp.2006.12.004.
[40] R.L.S. Ferreira, M.A.S. Anjos, A.K.C. Nóbrega, J.E.S. Pereira, E.F. Ledesma, The role of powder content of the recycled aggregates of CDW in the behaviour of rendering mortars, Constr. Build. Mater. 208 (2019) 601–612, https://doi.org/10.1016/j.conbuildmat.2019.03.058.
[41] C. Neno, J.De Brito, R. Veiga, Using fine recycled concrete aggregate for mortar production, Mater. Res. 17 (1) (2014) 168–177, https://doi.org/10.1590/S1516-14392013005000164.
[42] Dhir, R.K.; de Brito, J.; Silva, R.V.; Lye, C.Q. , Use of Recycled Aggregates in Mortar, 2019. ⟨https://doi.org/10.1016/b978–0-08–100985-7.00006–6⟩.
[43] L.F. Jochem, C.A. Casagrande, J.C. Rocha, Effect of lead in mortars with recycled aggregate and lightweight aggregate, Constr. Build. Mater. 239 (2020), 117702, https://doi.org/10.1016/J.CONBUILDMAT.2019.117702.
[44] UNE-EN 13139:2003, Áridos Para Morteros, Aenor, Madrid, España, 2003.
[45] UNE-EN 197–1, 2011, Cemento. Parte 1: Composición, Especificaciones y Criterios de Confromidad de Los Cementos Comunes, Aenor, Madrid, España, 2011.
[46] UNE-EN 196–3, 2017, Métodos de Ensayo de Cementos, Parte 3: Determinación Del Tiempo de Fraguado y de La Estabilidad de Volumen, 2017.
[47] UNE-EN 196–1, 2018, Métodos de Ensayo de Cementos. Parte 1: Determinación de Resistencias, Aenor, Madrid, España, 2018.
[48] UNE-EN 933–2,1996, Ensayos Para Determinar Las Propiedades Geométricas de Los Áridos. Parte 2: Determinación de La Granulometría de Las Partículas. Tamices de Ensayo, Tamaño Nominal de Las Aberturas, Aenor, Madrid, España, 1996.
[49] UNE-EN 933–1, 2012, Ensayos Para Determinar Las Propiedades Geométricas de Los Áridos. Parte 1: Determinación de La Granulometría de Las Partículas. Método Del Tamizado, Aenor, Madrid, España, 2012.
[50] P. Saiz Martínez, M. González Cortina, F. Fernández Martínez, A. Rodríguez Sánchez, Comparative Study of three types of fine recycled aggregates from construction and demolition waste (CDW), and their use in masonry mortar fabrication, J. Clean. Prod. 118 (2016) 162–169, https://doi.org/10.1016/j.jclepro.2016.01.059.
[51] EHE-08. Instrucción de Hormigón Estructural. Ministerio de Fomento. España. ⟨https://www.fomento.gob.es/organos-colegiados/mas-organos-colegiados/comision-permanente-del-hormigon/cph/instrucciones/ehe-08-version-en-castellano⟩. (Accessed 8 May 2019).
[52] UNE-EN 933–3, 2012, Ensayos Para Determinar Las Propiedades Geométricas de Los Áridos. Parte 3: Determinación de La Forma de Las Partículas. Índice de Lajas, Aenor, Madrid, España, 2012.
[53] UNE-EN 1097–6, 2014, Ensayos Para Determinar Las Propiedades Mecánicas y Físicas de Los Áridos. Parte 6: Determinación de La Densidad de Partículas y La Absorción de Agua. Aenor, Madrid, España, 2014.
[54] UNE-EN 1015-3:2000/A2:2007, Métodos de Ensayo Para Morteros de Albañilería. Parte 3: Determinación de La Consistencia Del Mortero Fresco (Por La Mesa de Sacudidas), Aenor, Madrid, España, 2007.
[55] C.-C. Fan, R. Huang, H. Hwang, S.-J. Chao, The Effects of different fine recycled concrete aggregates on the properties of mortar, Mater. (Basel) 8 (5) (2015) 2658–2672, https://doi.org/10.3390/MA8052658.
[56] R.V. Silva, J. de Brito, R.K. Dhir, Performance of cementitious renderings and masonry mortars containing recycled aggregates from construction and demolition wastes, Constr. Build. Mater. 105 (2016) 400–415, https://doi.org/10.1016/J.CONBUILDMAT.2015.12.171&QID=2&DOC=65&RECORDID=&COLNAME=WOS.
[57] R. Martínez-García, I.M. Guerra-Romero, J.M. Morán-del Pozo, J. de Brito, A. Juan-Valdés, Recycling aggregates for self-compacting concrete production: a feasible option, in: Materials, 13, 2020, https://doi.org/10.3390/ma13040868.
[58] R. Martínez-García, M.I.S. Rojas, J.M.M. de; Pozo, F.J. Fraile-Fernández, A. Juan-Valdés, Evaluation of mechanical characteristics of cement mortar with fine recycled concrete aggregates (FRCA), Sustainability 13 (1) (2021) 414, https://doi.org/10.3390/su13010414.
[59] V. Corinaldesi, G. Moriconi, Behaviour of cementitious mortars containing different kinds of recycled aggregate, Constr. Build. Mater. 23 (1) (2009) 289–294, https://doi.org/10.1016/j.conbuildmat.2007.12.006.
[60] M.T. Le, C. Tribout, G. Escadeillas, Durability of mortars with leftover recycled sand, Constr. Build. Mater. 215 (2019) 391–400, https://doi.org/10.1016/J.CONBUILDMAT.2019.04.179.
[61] UNE-EN 1015–10:2000/A1:2007, Métodos de Ensayo de Los Morteros Para Albañilería. Parte 10: Determinación de La Densidad Aparente En Seco Del Mortero Endurecido, Aenor, Madrid, España, 2007.
[62] Bonifazi, G.; Capobianco, G.; Serranti, S.; Eggimann, M.; Wagner, E.; Di Maio, F.; Lotfi, S. , The ITZ in Concrete with Natural and Recycled Aggregates: Study of Microstructures Based on Image and SEM Analysis, Delft University of Technology,17 2015.
[63] R. Maddalena, K. Li, P.A. Chater, S. Michalik, A. Hamilton, Direct synthesis of a solid calcium-silicate-hydrate (C-S-H), Constr. Build. Mater. 223 (2019) 554–565, https://doi.org/10.1016/j.conbuildmat.2019.06.024.
[64] UNE-EN 1015–18, Métodos de Ensayo de Los Morteros Para Albañilería. Parte 18: Determinación Del Coeficiente de Absorción de Agua Por Capilaridad Del Mortero Endurecido. Aenor, Madrid, España, 2003.
[65] UNE 83980, Durabilidad Del Hormigón. Métodos de Ensayo. Determinación de La Absorción de Agua, La Densidad y l Aporosidad Accesible Al Agua Del Hormigón, Aenor, Madrid, España, 2014.
[66] N. Hearn, R.D. Hooton, Sample mass and dimension effects on mercury intrusion porosimetry results, Cem. Concr. Res. 22 (5) (1992) 970–980, https://doi.org/10.1016/0008-8846(92)90121-B.
[67] M.J. Chinchillas-Chinchillas, M.J. Pellegrini-Cervantes, A. Castro-Beltrán, M. Rodríguez-Rodríguez, V.M. Orozco-Carmona, H.J. Peinado-Guevara, Properties of mortar with recycled aggregates, and polyacrylonitrile microfibers synthesized by electrospinning, Materials 12 (23) (2019) 3849, https://doi.org/10.3390/ma12233849.

[68] H. Donza, O. Cabrera, E.F. Irassar, High-strength concrete with different fine aggregate, Cem. Concr. Res. 32 (11) (2002) 1755–1761, https://doi.org/10.1016/S0008-8846(02)00860-8.
[69] Quiroga, P.N.; Fowler, D.W. , The Effects of Aggregates Characteristics on the Performance of Portland Cement Concrete 6. Performing Organization Code, 2004.
[70] Zhao, H.; Xiao, Q.; Huang, D.; Zhang, S.; Cheng, X.; Rodríguez-Castellanos, A.; Zheng, J. , Influence of Pore Structure on Compressive Strength of Cement Mortar, 2014. ⟨https://doi.org/10.1155/2014/247058⟩.
[71] M.S. de Juan, P.A. Gutiérrez, Study on the influence of attached mortar content on the properties of recycled concrete aggregate, Constr. Build. Mater. 23 (2) (2009) 872–877, https://doi.org/10.1016/j.conbuildmat.2008.04.012.
[72] M.T. Le, C. Tribout, G. Escadeillas, Durability of mortars with leftover recycled sand, Constr. Build. Mater. 215 (2019) 391–400, https://doi.org/10.1016/j.conbuildmat.2019.04.179.
[73] A.K. Padmini, K. Ramamurthy, M.S. Mathews, Influence of parent concrete on the properties of recycled aggregate concrete, Constr. Build. Mater. 23 (2) (2009) 829–836, https://doi.org/10.1016/j.conbuildmat.2008.03.006.
[74] L.F. Jochem, C.A. Casagrande, J.C. Rocha, Effect of Lead in mortars with recycled aggregate and lightweight aggregate, Constr. Build. Mater. 239 (2020), 117702, https://doi.org/10.1016/j.conbuildmat.2019.117702.
[75] D. Zou, K. Wang, K. Li, W. Ruan, P. Liu, Y. Zhu, Does enhanced hydration have impact on autogenous deformation of internally cued mortar? Constr. Build. Mater. 209 (2019) 548–554, https://doi.org/10.1016/j.conbuildmat.2019.03.165.
[76] Mehta, P.K.; Monteiro, P.J. M. , Concrete Microstructure, Properties, and Materials, McGraw-Hill, Ed, third ed., McGraw-Hill; Scientific Research Publishing, New York, 2006.
[77] Z. Li, Advanced Concrete Technology, John Wiley & Sons, Inc., Canada, 2011.
[78] A. Silva, R. Neves, J. De Brito, Statistical modelling of carbonation in reinforced concrete, Cem. Concr. Compos. 50 (2014) 73–81, https://doi.org/10.1016/j.cemconcomp.2013.12.001.
[79] V.W.Y. Tam, X.F. Gao, C.M. Tam, Microstructural analysis of recycled aggregate concrete produced from two-stage mixing approach, Cem. Concr. Res. 35 (6) (2005) 1195–1203, https://doi.org/10.1016/j.cemconres.2004.10.025.
[80] R. Martínez-García, P. Jagadesh, F.J. Fraile-Fernández, J.M.M. Pozo, Del, A. Juan-Valdés, Influence of design parameters on fresh properties of self-compacting concrete with recycled aggregate—a review, Materials 2 (2020) 1–24, https://doi.org/10.3390/ma13245749.
[81] S. Diamond, K.O. Kjellsen, Resolution of fine fibrous C-S-H in backscatter SEM examination, Cem. Concr. Compos. 28 (2) (2006) 130–132, https://doi.org/10.1016/j.cemconcomp.2005.10.002.
[82] H. Manzano, J.S. Dolado, M. Griebel, J. Hamaekers, A molecular dynamics study of the aluminosilicate chains structure in Al-Rich calcium silicate hydrated (C-S-H) gels, Phys. Status Solidi A Appl. Mater. Sci. 205 (2008) 1324–1329, https://doi.org/10.1002/pssa.200778175.
[83] I.G. Richardson, J.G. Cabrera, Nature of C-S-H in model slag-cements, Cem. Concr. Compos 22 (4) (2000) 259–266, https://doi.org/10.1016/S0958-9465(00)00022-6.
[84] W. Kunther, S. Ferreiro, J. Skibsted, Influence of the Ca/Si ratio on the compressive strength of cementitious calcium-silicate-hydrate binders, J. Mater. Chem. A 5 (33) (2017) 17401–17412, https://doi.org/10.1039/c7ta06104h.
[85] C. Famy, A.R. Brough, H.F.W. Taylor, The C-S-H gel of portland cement mortars: Part I. the interpretation of energy-dispersive X-ray microanalyses from scanning electron microscopy, with some observations on C-S-H, AFm and AFt phase compositions, Cem. Concr. Res. 33 (9) (2003) 1389–1398, https://doi.org/10.1016/S0008-8846(03)00064-4.
[86] M. Lenart, Impact assessment of lime additive and chemical admixtures on selected properties of mortars, Procedia Eng. 57 (2013) 687–696, https://doi.org/10.1016/j.proeng.2013.04.087.
[87] A. Yacoub, A. Djerbi, T. Fen-Chong, Water absorption in recycled sand: new experimental methods to estimate the water saturation degree and kinetic filling during mortar mixing, Constr. Build. Mater. 158 (2018) 464–471, https://doi.org/10.1016/j.conbuildmat.2017.10.023.
[88] A. Katz, D. Kulisch, Performance of mortars containing recycled fine aggregate from construction and demolition waste, Mater. Struct. Constr. 50 (4) (2017), https://doi.org/10.1617/s11527-017-1067-x.
[89] J. De Brito, F. Alves, Concrete with recycled aggregates: the portuguese experimental research, Mater. Struct. Constr. 43 (SUPPL. 1) (2010) 35–51, https://doi.org/10.1617/s11527-010-9595-7.
[90] R. Raeis Samiei, B. Daniotti, R. Pelosato, G. Dotelli, Properties of cement-lime mortars vs. cement mortars containing recycled concrete aggregates, Constr. Build. Mater. 84 (2015) 84–94, https://doi.org/10.1016/j.conbuildmat.2015.03.042.
[91] J. García-González, D. Rodríguez-Robles, A. Juan-Valdés, J.M. Morán-del Pozo, M.I. Guerra-Romero, Porosity and pore size distribution in recycled concrete, Mag. Concr. Res. 67 (22) (2015) 1214–1221, https://doi.org/10.1680/macr.14.00218.
[92] V.W.Y. Tam, C.M. Tam, K.N. Le, Removal of cement mortar remains from recycled aggregate using pre-soaking approaches, Resour. Conserv. Recycl. 50 (1) (2007) 82–101, https://doi.org/10.1016/j.resconrec.2006.05.012.
[93] R.A. Cook, K.C. Hover, Mercury porosimetry of hardened cement pastes, Cem. Concr. Res. 29 (6) (1999) 933–943, https://doi.org/10.1016/S0008-8846(99)00083-6.
[94] M. O'Farrell, S. Wild, B.B. Sabir, Pore size distribution and compressive strength of waste clay brick mortar, Cem. Concr. Compos. 23 (1) (2001) 81–91, https://doi.org/10.1016/S0958-9465(00)00070-6.
[95] R. Kumar, B. Bhattacharjee, Study on some factors affecting the results in the use of mip method in concrete research, Cem. Concr. Res. 33 (3) (2003) 417–424, https://doi.org/10.1016/S0008-8846(02)00974-2.
[96] X. Hu, C. Shi, Z. Shi, L. Zhang, Compressive strength, pore structure and chloride transport properties of alkali-activated slag/fly ash mortars, Cem. Concr. Compos. 104 (2019), 103392, https://doi.org/10.1016/j.cemconcomp.2019.103392.
[97] Shi, C.; Tang, X.; Li, Y. , Studies on the activation of phosphorus slag, in: Proceedings of the Third International Conference on the Use of Fly Ash, Silica Fume, Slag and Natural Pozzolans in Concrete, 1989, 657–666.
[98] Kendall, K.; Howard, A.J.; Birchall, J.D. , relation between porosity, microstructure and strength, and the approach to advanced cement-based materials, Philos. Trans. R. Soc. Lond. Ser. A, Math. Phys. Sci., 1983, 139–153. ⟨https://doi.org/10.1098/rsta.1983.0073⟩.
[99] P. Mangat, P. Lambert, Sustainability of alkali-activated cementitious materials and geopolymers. Sustainability of Construction Materials, Elsevier,, 2016, pp. 459–476, https://doi.org/10.1016/b978-0-08-100370-1.00018-4.
[100] M.Y. Balshin, Relation of mechanical properties of powder metals and their porosity and the ultimate properties of porous metal-ceramic materials, Dokl. Akad. Nauk SSSR 57 (5) (1949) 831–834.
[101] R. R, Compression strength of porous sintered alumina zirconia, J. Am. Ceram. Soc. 36 (2) (1953) 65–68.
[102] K. Schiller, Strength of porous materials, Cem. Concr. Res. 1 (1971) 419–422.
[103] D. Hasselman, On the porosity dependence of the elastic moduli of polycrystalline refractory materials, J. Am. Ceram. Soc. 45 (1962) 452–453.